NASA CR-132263

GaN FOR LED APPLICATIONS

by

J. I. PANKOVE

FINAL REPORT

MAY 1973

PREPARED UNDER CONTRACT NO. NAS1-11553

RCA LABORATORIES
PRINCETON, NJ 08540

LANGLEY RESEARCH CENTER
NATIONAL AERONAUTICS AND SPACE ADMINISTRATION
HAMPTON, VA 23365

Roger Breckenbridge
Technical Monitor

NAS1-11553
Langley Research Center
NATIONAL AERONAUTICS AND SPACE ADMINISTRATION
Hampton, VA 23365

Requests for copies of this report should be referred to:

NASA Scientific and Technical Information Facility
P. O. Box 33
College Park
Maryland 20740

1. Report No.	2. Government Accession No.	3. Recipient's Catalog No.
NASA CR-132263		

4. Title and Subtitle	5. Report Date
GaN for LED Applications	May 1973
	6. Performing Organization Code

7. Author(s)	8. Performing Organization Report No.
J. I. Pankove	PRRL-73-CR-32

9. Performing Organization Name and Address	10. Work Unit No.
RCA Laboratories Princeton, New Jersey 08540	11. Contract or Grant No. NAS1-11553
	13. Type of Report and Period Covered Final Report 4/18/72 to 4/17/73
12. Sponsoring Agency Name and Address Langley Research Center Hampton, VA 23365	14. Sponsoring Agency Code

15. Supplementary Notes

16. Abstract

In order to improve the synthesis of GaN the effect of various growth and doping parameters has been studied. Although Be, Li, Mg, and Dy can be used to overcompensate native donors, the most interesting acceptor element is Zn. The emission spectrum and the luminescence efficiency depend on the growth temperature (below 800°C), on the partial pressure of the doping impurity, and on the duration of growth. Blue-green electroluminescence with a power efficiency of 0.1% and a brightness of 850 fL (at 0.6 mA and 22.5 V) has been obtained. Some diodes allow to change the color of the emitted light by reversing the polarity of the bias. Continuous operation of a diode over a period of 5 months showed no evidence of degradation. The luminescence properties of ion-implanted GaN were studied. Delay effects were found in the electroluminescence of diodes, although, with a dc bias, a 70-MHz modulation was possible. Further progress will require the evolution of a satisfactory theoretical model, an improvement in the substrate to minimize interfacial strains, and the search for a shallow acceptor impurity to obtain p-type GaN.

17. Key Words (Selected by Author(s))	18. Distribution Statement
Electroluminescence Luminescence GaN	

19. Security Classif. (of this report)	20. Security Classif. (of this page)	21. No. of Pages	22. Price*
Unclassified	Unclassified	64	

*For sale by National Technical Information Service, Springfield, Virginia 22151.

TABLE OF CONTENTS

TABLE OF CONTENTS (Continued)

LIST OF ILLUSTRATIONS

LIST OF ILLUSTRATIONS (Continued)

LIST OF ILLUSTRATIONS (Continued)

LIST OF TABLES

GaN FOR LED APPLICATIONS

by

J. I. Pankove

RCA Laboratories

Princeton, New Jersey 08540

SUMMARY

In order to improve the synthesis of GaN the effect of various growth and doping parameters has been studied. Although Be, Li Mg, and Dy can be used to overcompensate native donors, the most interesting acceptor element is Zn. The emission spectrum and the luminescence efficiency depend on the growth temperature (below 800°C), on the partial pressure of the doping impurity, and on the duration of growth. Blue-green electroluminescence with a power efficiency of 0.1% and a brightness of 850 fL (at 0.6 mA and 22.5 V) has been obtained. Some diodes allow to change the color of the emitted light by reversing the polarity of the bias. Continuous operation of a diode over a period of 5 months showed no evidence of degradation. The luminescence properties of ion-implanted GaN were studied. Delay effects were found in the electroluminescence of diodes, although, with a dc bias, a 70-MHz modulation was possible. Further progress will require the evolution of a satisfactory theoretical model, an improvement in the substrate to minimize interfacial strains, and the search for a shallow acceptor impurity to obtain p-type GaN.

I. INTRODUCTION

The objective of this research was to improve the synthesis of GaN and to learn how to dope this material controllably, with the ultimate goal of generating a semiconductor with p-type conduction. It was expected that in this direct gap material efficient electroluminescence should be obtained in the near UV and in the visible. Injection electroluminescence from a pn junction was therefore the final aim of this program.

Our approach was first to study carefully the various parameters which are critical to the generation of high quality material. Various dopants were tried. Zn was the most promising acceptor-like impurity. Although type conversion was not achieved, complete compensation of native donors was obtained and the material became insulating. Even though a pn junction was not realized, bright electroluminescence was obtained with compensated GaN in that portion of the visible spectrum which is the most interesting for practical applications, namely in the blue-green. Much effort was then devoted to optimizing those parameters which lead to improved performance of GaN light-emitting diodes (LEDs). In particular, we studied the incorporation of Zn during vapor growth, by diffusion, and by ion implantation. We found some advantage in annealing the material to reduce mechanical strains.

Novel test facilities were designed to facilitate the characterization of the diodes. All this effort culminated in a 0.1% efficient blue-green LED, operating continuously at room temperature and having a luminance of 850 fL, capable of 50-MHz modulation and having a continuously operating life in excess of 5 months.

Finally, the attention was turned to an in-depth understanding of the mechanisms involved in the electroluminescence of insulating GaN. It is hoped that this understanding will not only permit additional breakthroughs in the performance of GaN LEDs but that it will also explain the long elusive mechanism of electroluminescence in other compounds such as ZnS.

The research to be described below was only partly supported by this contract, most of the funding coming from RCA.

II. REVIEW OF WORK DONE PRIOR TO THIS CONTRACT

The growth technique used to prepare the GaN layers was developed and reported under NASA Contract No. 12-538. This synthesis method, now known as the Maruska-Tietjen vapor phase method (ref.1), produced large-area single crystals exhibiting efficient near-gap luminescence (ref. 2). Our measurement of the absorption edge (ref. 3) indicated (in spite of a systematic error in the absolute value of the absorption coefficient) (ref. 4) that GaN has a direct gap of 3.50 eV. This conclusion was confirmed by S. Bloom's (ref. 5) band structure calculations at RCA Laboratories and by other observations (refs. 4, 6). The actual absorption spectrum consists of four regions illustrated schematically in Fig. 1 and summarized briefly below:

(1) For photon energy less than about 1.5 eV, the dominant mechanism involves free carrier absorption which varies as $h\nu^{-n}$. n is in the range of 2.5 to 3.9, depending on the doping (ref. 7).
(2) In the region where $1.7 < h\nu < 3.0$ eV, the absorption coefficient varies as $(h\nu - 1.7)^2$, corresponding to a transition involving a deep center in the middle of the gap.
(3) Between 3.0 and 3.3 eV, the absorption coefficient varies exponentially with $h\nu$.
(4) Between 3.3 and 3.5 eV, a steeper exponential dependence is observed.

By separating the various components, it is possible to follow the temperature dependence of the energy gap which approximately parallels the shift of the fundamental absorption edge. This data is plotted in Fig. 2. In the linear region above 140 K, $dE_g/dT = -4.8 \times 10^{-4}$ eV/K. The details of the absorption data summarized above will be published when the experimental work is completed.

UV reflectance spectroscopy (ref. 8) at our laboratory in Zurich* has provided fiduciary points for band structure calculations (ref. 5), the results of which indicate that the indirect valleys are at a very high potential (about 3 eV) above the conduction band minimum at the Γ center of symmetry (Fig. 3).

The anomalous dispersion of IR reflectance near the plasma frequency was measured (ref. 9). However, to determine the carrier effective mass from IR reflectance data one must know the carrier scattering time.

---

*Laboratories RCA, Ltd., Zurich, Switzerland.

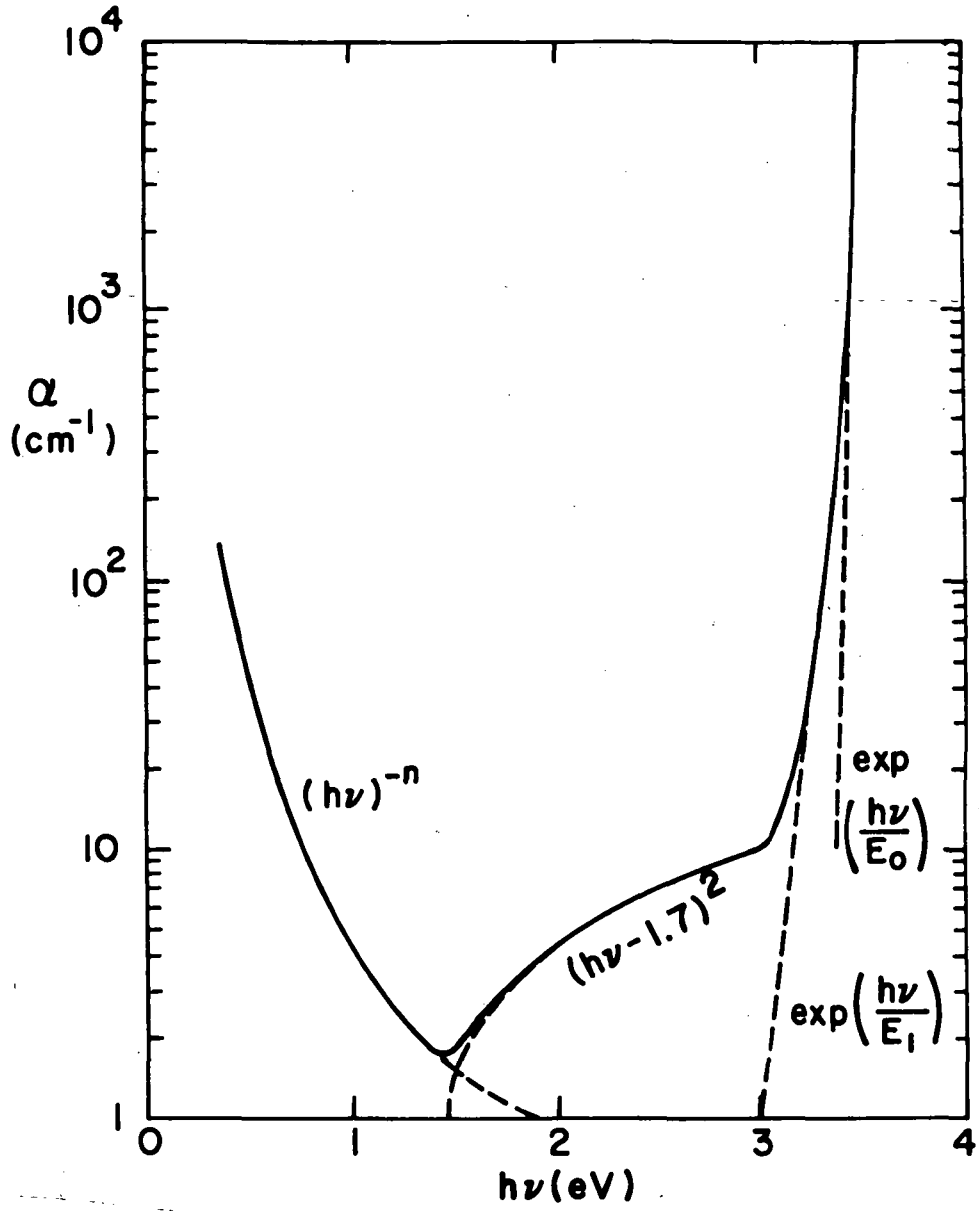

Figure 1. Schematized optical absorption of GaN.

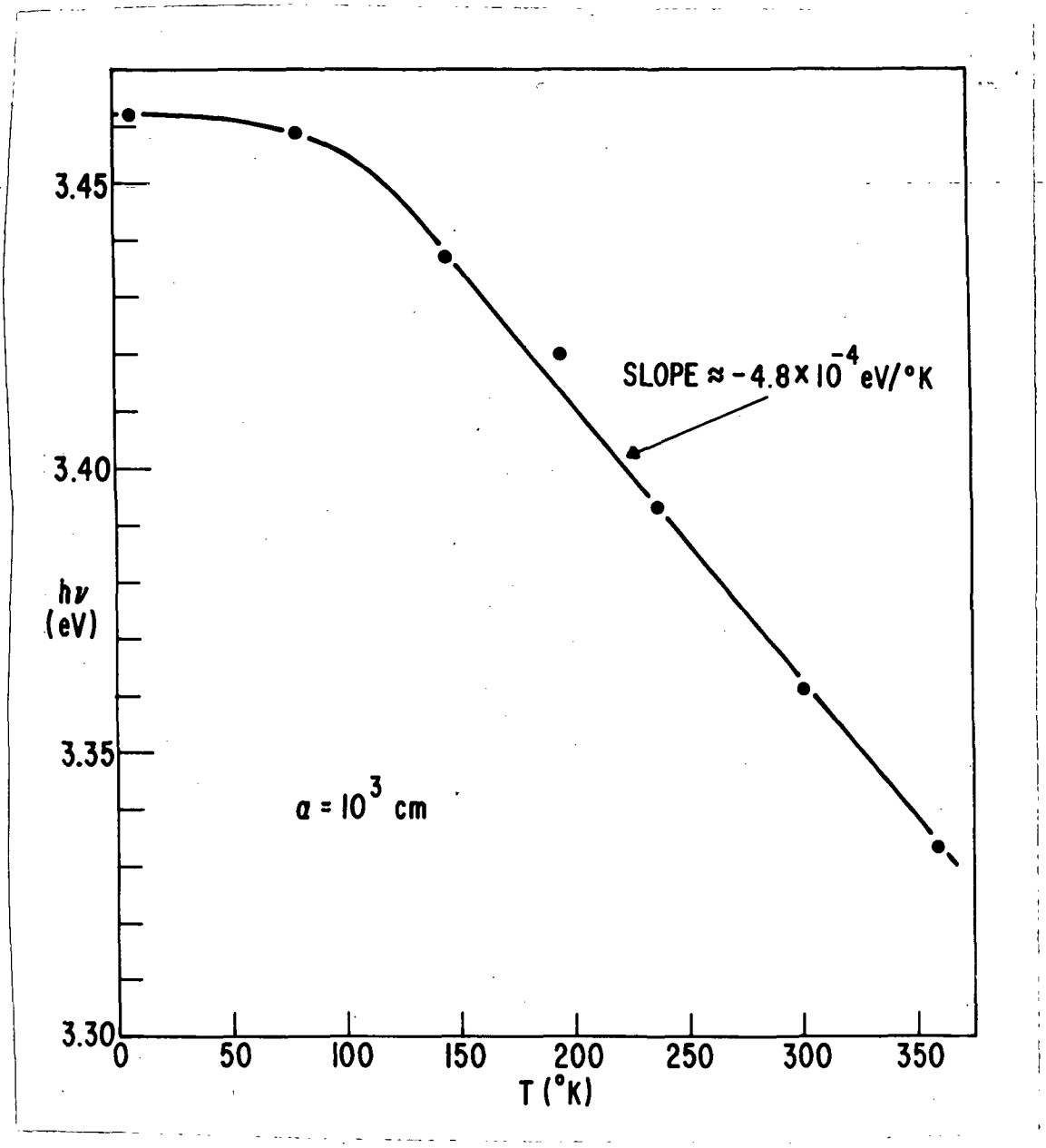

Figure 2. Temperature dependence of the absorption edge of GaN at $\alpha = 10^3$ cm.

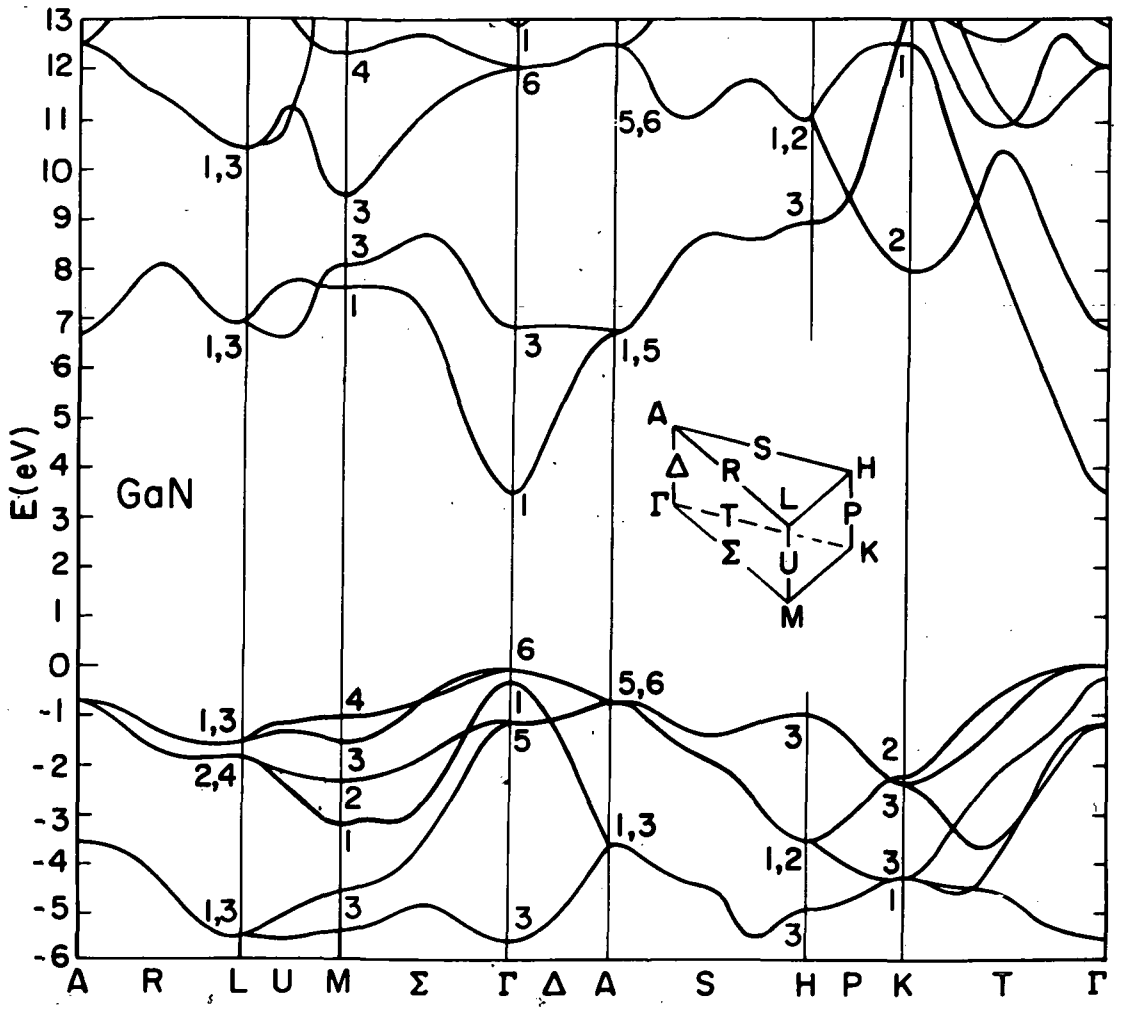

Figure 3. Band structure of GaN [courtesy of S. Bloom (ref. 5)].

Undoped GaN is always n-type and highly conducting. It was soon found that Zn compensates the native donors, making the material insulating, and allows the observation of dc electroluminescence (ref. 10). Further experiments with Zn doping in LED structures revealed the possibility of getting blue (ref. 11), green (ref. 12), yellow or red (ref. 13) emission - these are shown in Fig. 4.

UV electroluminescence has been obtained in undoped GaN by the following two techniques. In the first method (ref. 14), a surface barrier (perhaps a Schottky barrier) is made under a dot of colloidal carbon ("Aquadag"). In this case, dc UV electroluminescence peaking at 3.22 eV has been obtained - curve E in Fig. 4. In the second

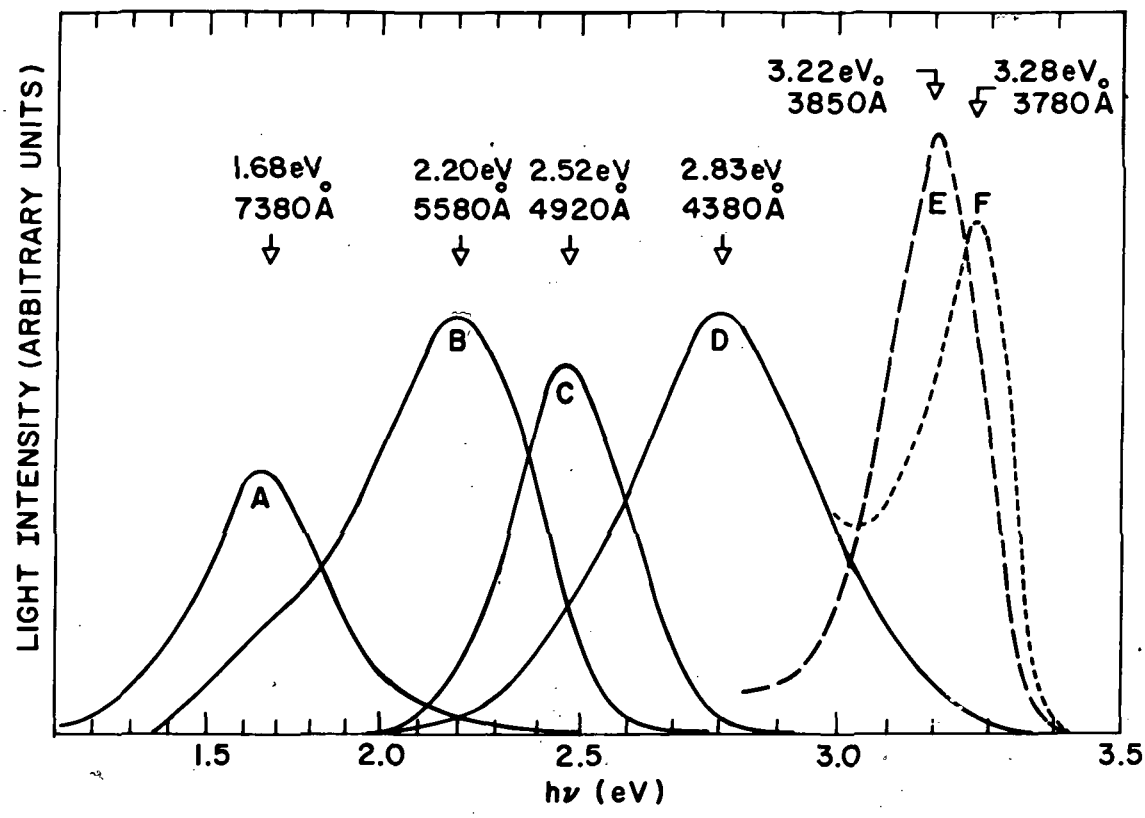

Figure 4. Emission spectra of various GaN LED's. Solid lines are for i-n structures using Zn-doped material. Dashed and dotted lines are for diodes made on undoped GaN.

approach (ref. 15), a metal-insulator-semiconductor (MIS) structure is fabricated. First, a negative pulse is applied across the device to produce a surface inversion layer (rendering the surface quasi-p-type); then a positive pulse is used to inject the surface holes into the n-type bulk where radiative recombination occurs, emitting ultraviolet radiation at about 3800 Å - curve F in Fig. 4.

Because of a mismatch between the lattices of the GaN and of the sapphire substrate, and also because of the differences in the coefficients of thermal expansion for these two materials, severe strains are generated at the sapphire-GaN interface. These strains create dislocations and other crystal imperfections, which can be efficient centers for nonradiative recombination. Some of these imperfections can be annealed if the GaN is separated from the substrate. Fortunately, we have developed an etching technique (ref. 16) which can remove preferentially the n-type layer. Thus, the Zn-doped insulating layer

can be made free of the substrate and self-supporting. This unconstrained material is then annealed in ammonia to prevent the decomposition of GaN. Photoluminescence measurements were made on such a specimen at 78 K at various stages of the annealing treatment. The results shown in Fig. 5 indicate that the photoluminescence efficiency increases by a factor of about four when the specimen is annealed above 1000°C. No further improvement is obtained beyond 1050°C. Initially and after each annealing step, the 78 K photoluminescence spectrum peaked in the blue at 2.88 eV.

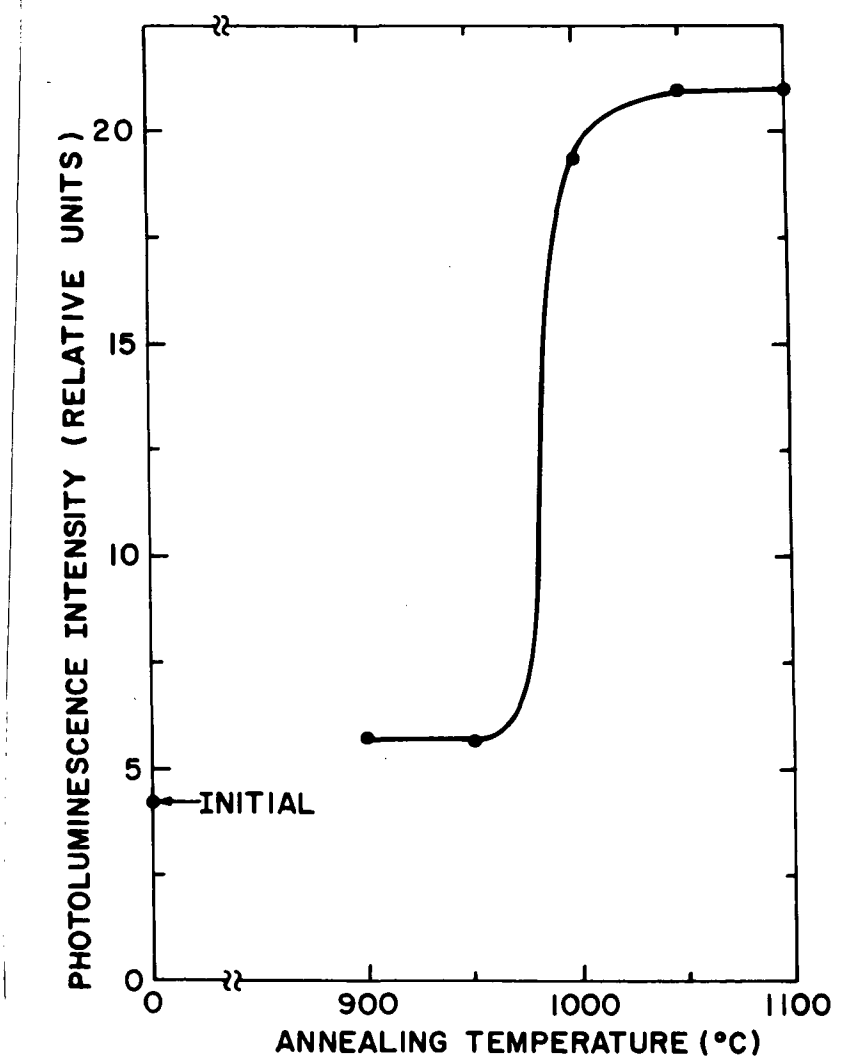

Figure 5. Photoluminescence intensity of self-supporting Zn-doped GaN after annealing in ammonia for 1/2 hour at the indicated temperatures.

III. MATERIAL SYNTHESIS

GaN was synthesized from GaCl and ammonia by the Maruska-Tietjen method (ref. 1). Volatile monochloride of gallium is formed by passing HCl in a H_2 carrier gas over hot liquid Ga. This is then mixed with ammonia, and the mixture is passed over a substrate where epitaxial growth occurs. A schematic diagram of the apparatus is shown in Fig. 6.

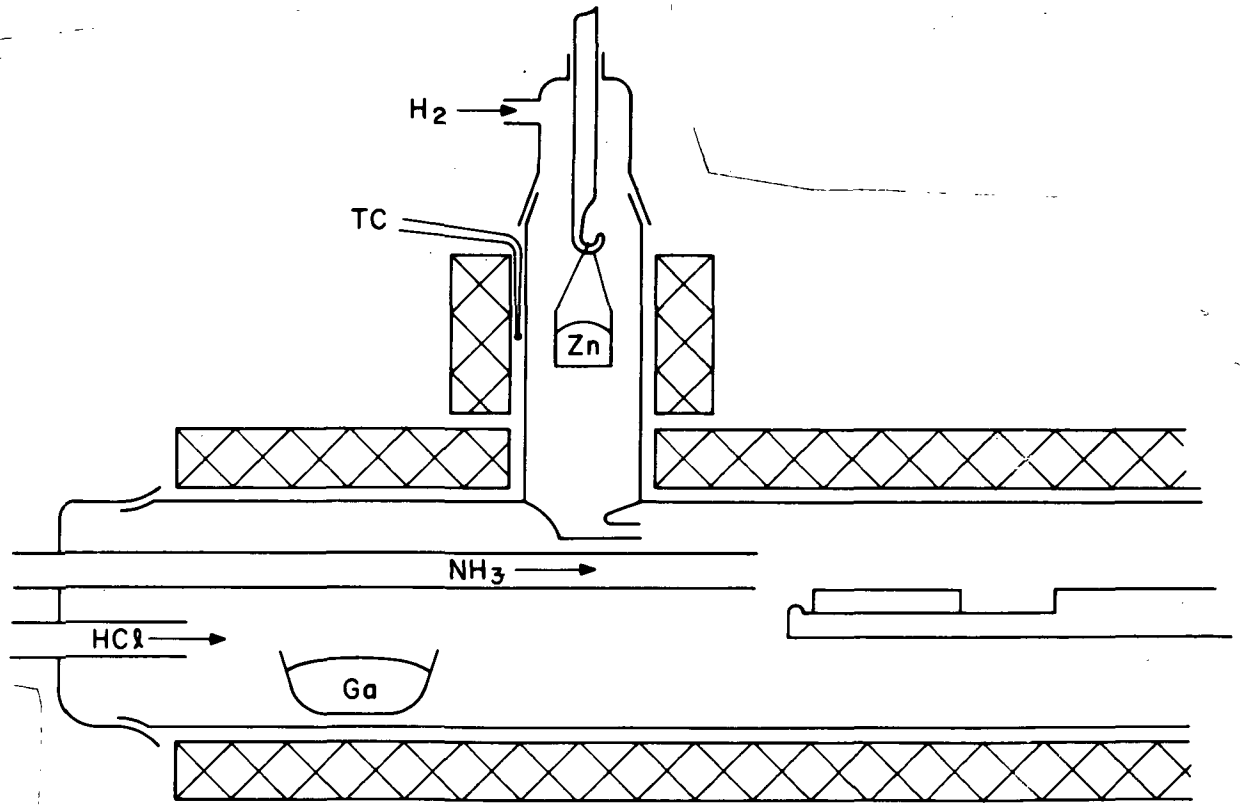

Figure 6. Furnace for growing GaN.

Typically, the temperature of the reactor is about 950°C. Also shown in Fig. 6 is the sidearm used for introducing dopants during growth.

The growth of GaN differs from the growth of other III-V compounds in that at the temperature of growth, GaN is unstable and decomposes via the reaction:

$$GaN \rightarrow Ga_{(\ell)} + 1/2N_{2(g)} \qquad (1)$$

However, the reaction:

$$GaCl_{(g)} + NH_{3(g)} \rightarrow GaN_{(s)} + HCl_{(g)} + H_{2(g)} \quad (2)$$

is much faster than the decomposition reaction and therefore growth occurs (ref. 17). Present best estimates of the dissociation pressure of GaN lead to N_2 pressures of about 1000 atm at 1000°C. It is believed that the residual donor concentration in as-grown GaN arises from its high concentration of nitrogen vacancies, again related to the high dissociation pressure at growth temperatures.

Another complication in the growth of GaN is related to the sensitivity of reaction (2) to the catalytic properties of the substrate surface. GaN and sapphire appear to be the most favorable surfaces for promoting reaction (2), whereas Si and GaP appear to be poor catalysts and therefore it is difficult to grow GaN on them. It is because of this catalytic effect that sapphire has been almost exclusively used as a substrate for GaN growth. However, sapphire does not match GaN in its lattice structure, lattice constant or coefficient of thermal expansion. The grown layers are highly strained. Upon cooling, the sapphire shrinks more than the GaN; hence, the wafers are usually concave on the sapphire side. Often, the sapphire, being under tension, fractures into many pieces that are held together by the GaN layer.

Although GaN should exist in a cubic form, as well as hexagonal, only the hexagonal form has been obtained. X-ray lines of the cubic form have been observed in some of the powder residues found in the reaction tubes, but crystals of this form have never been isolated from the mixture. We have grown GaN on other substrates which were expected to be better matches to GaN (tungsten, βSic, Zr, BP, and ZnO), but have always obtained polycrystalline layers of hexagonal GaN. In the case of ZnO, this substrate decomposed during growth, breaking up the GaN crust.

GaN has the Wurtzite crystal structure with lattice constants a = 3.18 Å and c = 5.18 Å (ref. 18). The cubic phase has a lattice constant of 4.51 Å (ref. 19).

After extensive experimentation with various flow rates, the following values were found to give the best results in terms of lowest electron concentration and highest mobility:

HCl 30 cc/min + H_2 300 cc/min
NH_3 3000 cc/min + H_2 300 cc/min
H_2 300 cc/min in sidearm

Although GaN has been grown at temperatures ranging from 750° to 1050°C, the furnace temperature was optimized at 950°C. The gallium is also held at 950°C, with one exception, to be discussed later. Only h the sidearm furnace temperature was varied, and this was done to control the vapor pressure of the dopant. The exception deals with the effect of growth temperature on Zn doping. At the lower temperatures, the material tends to be polycrystalline, whereas at the higher temperatures, the growth rate is reduced by favoring reaction (1).

The orientation of the sapphire substrate did not appear critical to the quality of the undoped GaN. However, the dependence of orientation on the performance of light-emitting diodes has not been studied. These were always grown on $1\bar{1}02$ sapphire.

IV. DOPING EXPERIMENTS

A. Berylium

The Be located in the sidearm of the furnace was exposed to a stream of HCl to produce a vapor of $BeCl_2$. The temperature of the Be source, T_{Be}, ranged from 400° to 900°C.

The incorporation of Be in GaN becomes noticeable as a drop in electron mobility when $T_{Be} > 500°C$. When T_{Be} exceeds 600°C, the resulting GaN becomes insulating at room temperature.

Photoluminescent spectra of this material were taken at room temperature and at liquid-nitrogen temperature using a UV HeCd laser as a source of excitation. Typical spectra are shown in Fig. 7. The spectra are

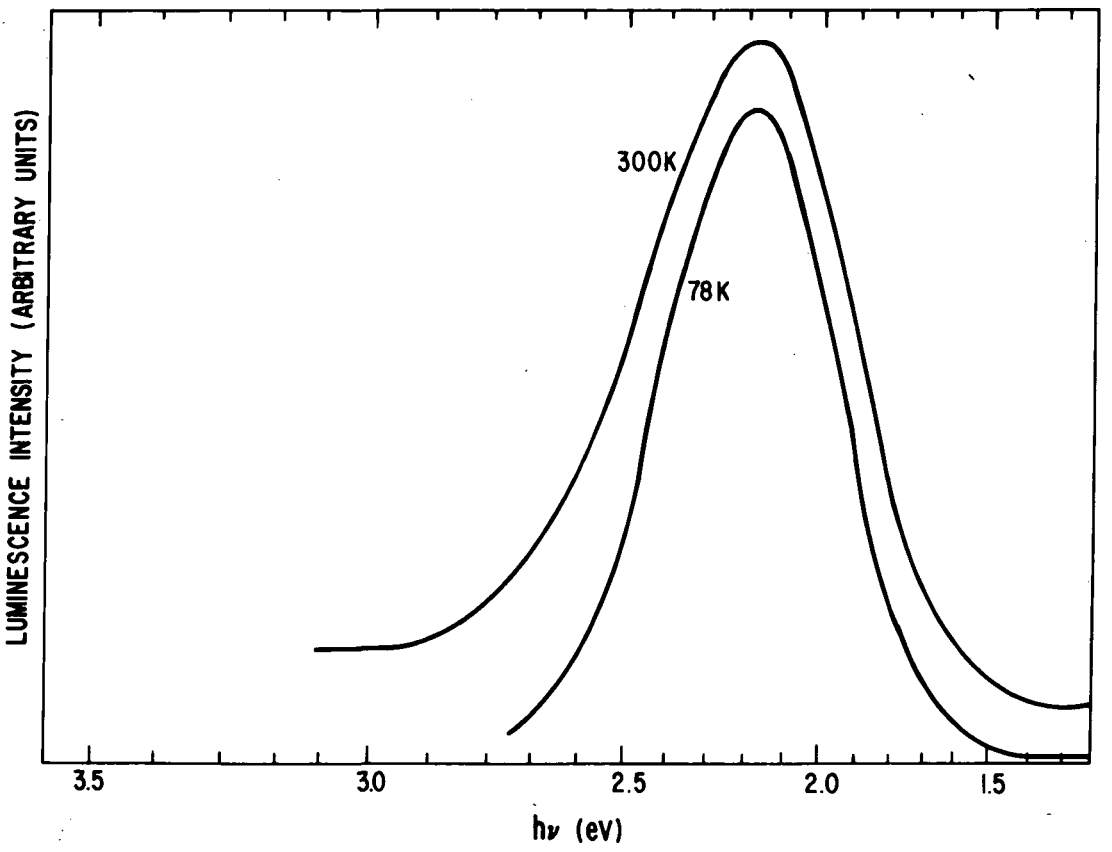

Figure 7. Photoluminescence spectra of Be-doped GaN.

characterized by a broad emission peaking at 2.16 ± 0.04 eV. It was noted in particular that the near-gap emission at about 3.47 eV (ref. 2) and the donor-acceptor pair recombination at 3.3 to 3.1 eV (ref. 6) were absent in most insulating Be-doped samples and very weak in other specimens. From this experiment, it is concluded that Be may form a deep center (probably a Be-N-vacancy complex) with a binding energy of 2.16 eV. Our results differ from those of Ilegems and Dingle (ref. 20) who find in semi-insulating Be-doped GaN a very pronounced near-gap peak, the intensity of which is comparable to that of the 2.16-eV peak, and a weaker donor-acceptor pair structure.

B. Cadmium

Blue photoluminescence, similar to that obtained with Zn, has been reported by Ilegems et al. (ref. 21) and had been observed in our earliest experiments with Cd which was found to contain a high concentration of Zn as an impurity (200 ppm).

For our most recent attempts, the Cd was analyzed and found to contain 5.2 ppm of Zn. The Cd source was operated in the range of 400° to 875°C, a range over which the vapor pressure of Cd is more than one order of magnitude greater than that of Zn (ref. 22). Material grown with source temperatures, $T_{Cd} > 600°C$, exhibited some blue photoluminescence and a dominant near-gap emission at 3.44 eV. This contrasts to the behavior of heavily Zn-doped material where only blue light is emitted and no near-gap component is present. A spectrometric analysis of the GaN revealed that there were 4.5 ppm Cd and 1.2 ppm Zn in the GaN. Hence we could conclude that the blue 2.75-eV emission is due to the presence of Zn in GaN. The furnace liner, which was coated with GaN during the Cd doping runs, exhibited photoluminescence peaks in order of decreasing intensity at 3.43, 3.32, 2.80, and 2.15 eV, as shown in Fig. 8.

Our results raise a serious doubt as to the previously published (ref. 21) interpretation of luminescence measurements in "Cd-doped" GaN.

C. Sodium

To dope GaN with sodium, the Na source was heated to temperatures, T_{Na}, ranging from 280° to 500°C. Although arc spectroscopy revealed up to 60 ppm concentration of Na in GaN, there was no other clear evidence for the presence of Na in the crystal: The carrier concentration and mobility remained substantially unaffected, and the emission spectrum

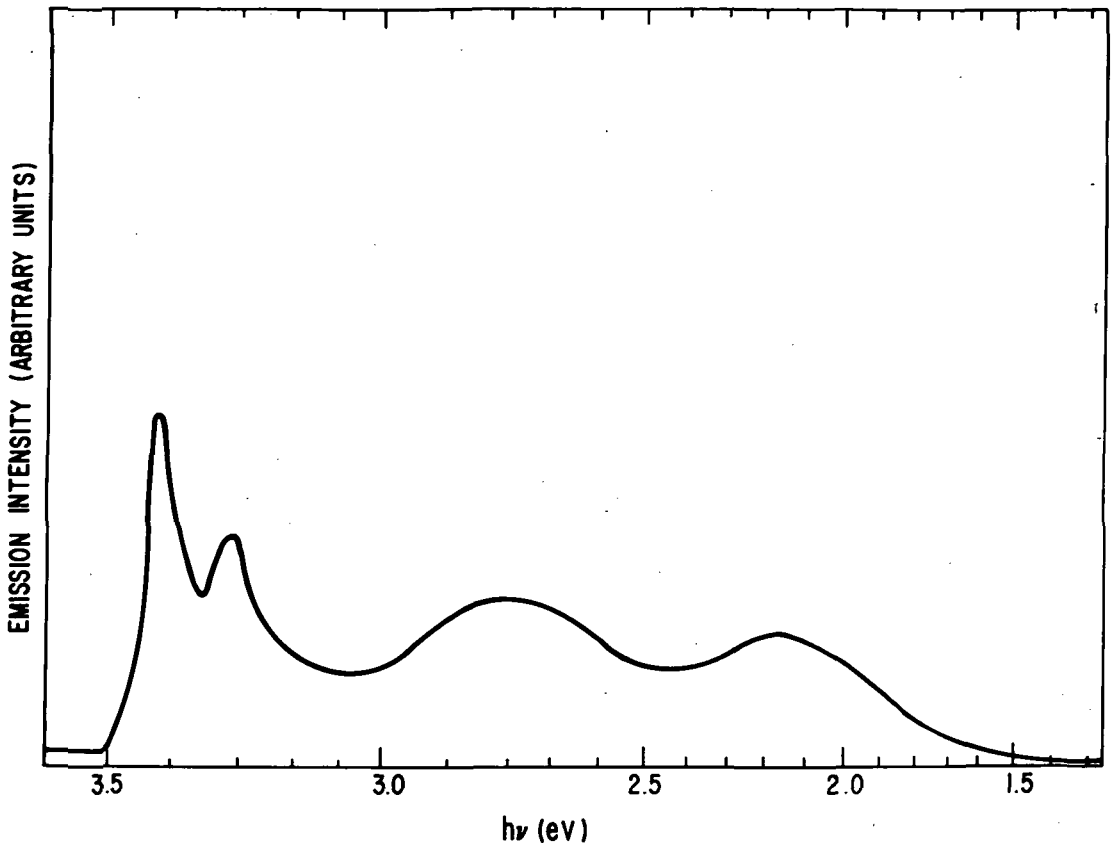

Figure 8. Photoluminescence spectrum of Cd-doped GaN (data taken at 78 K).

peaked mostly at 3.15 eV in a 0.4-eV-wide band at half maximum (Fig. 9). The peak coincides with the usual donor-acceptor transition (ref. 6). It must be pointed out that in our undoped GaN the donor-acceptor band is usually much weaker than the near-gap peak at 3.45 to 3.48 eV. Hence, it is conceivable that sodium might form a shallow acceptor which is over-compensated by donors (either the presumed N-vacancies or perhaps interstitial Na).

D. Calcium

Calcium was evaporated in the sidearm at a temperature, T_{Ca}, in the 800° to 900°C range. The resulting GaN contained several parts per

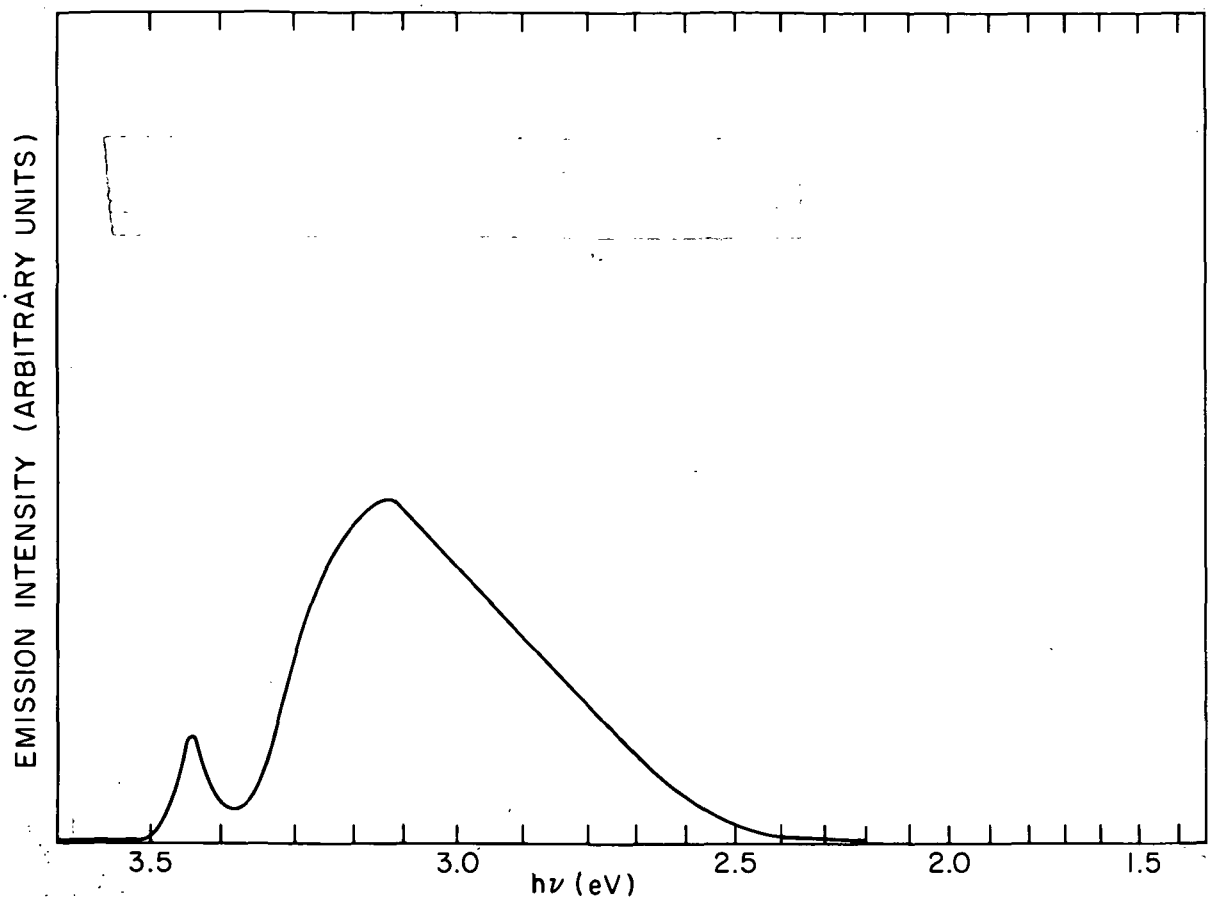

Figure 9. Photoluminescence spectrum of Na-doped GaN.

million of Ca. No effect was observed on the carrier concentration or the mobility. However, the photoluminescence spectrum exhibited a peak at about 2.9 eV (Fig. 10), which could be attributed to a radiative transition at a Ca center.

E. Dysprosium

HCl was passed over Dy in the sidearm at 800°C. The resulting GaN was semi-insulating and exhibited a broad photoluminescence peak

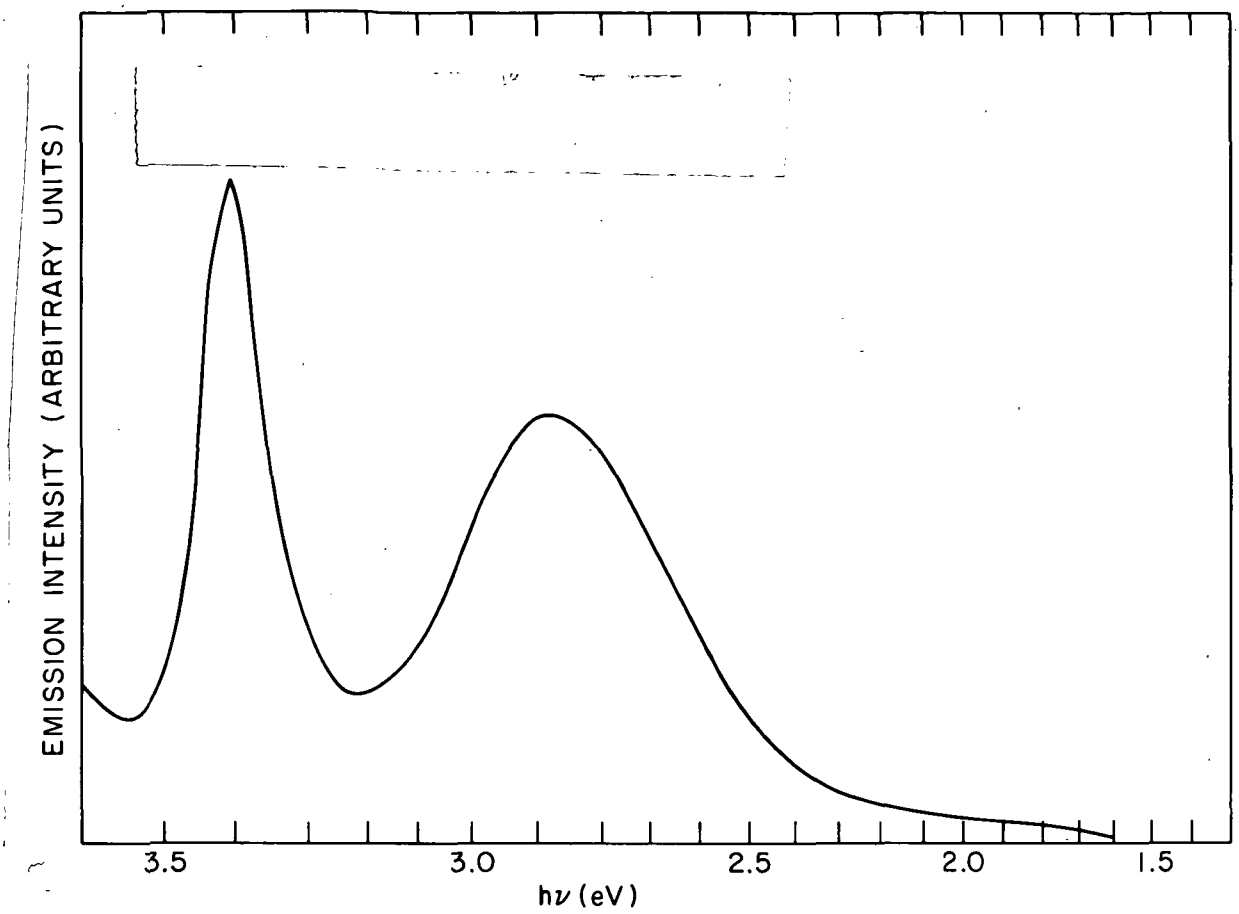

Figure 10. Photoluminescence spectrum of Ca-doped GaN.

at about 3.15 eV (Fig. 11). Since this emission falls in the range where one can obtain donor-acceptor recombination in undoped material, it may be too hasty to conclude that Dy is responsible for this peak. On the other hand, the absence of the near-gap emission strongly suggests that the capture cross section of Dy is the dominant factor in the pair recombination. Further study of this impurity is needed, especially in the infrared, since Dy should have a radiative transition at 2.5 μm.

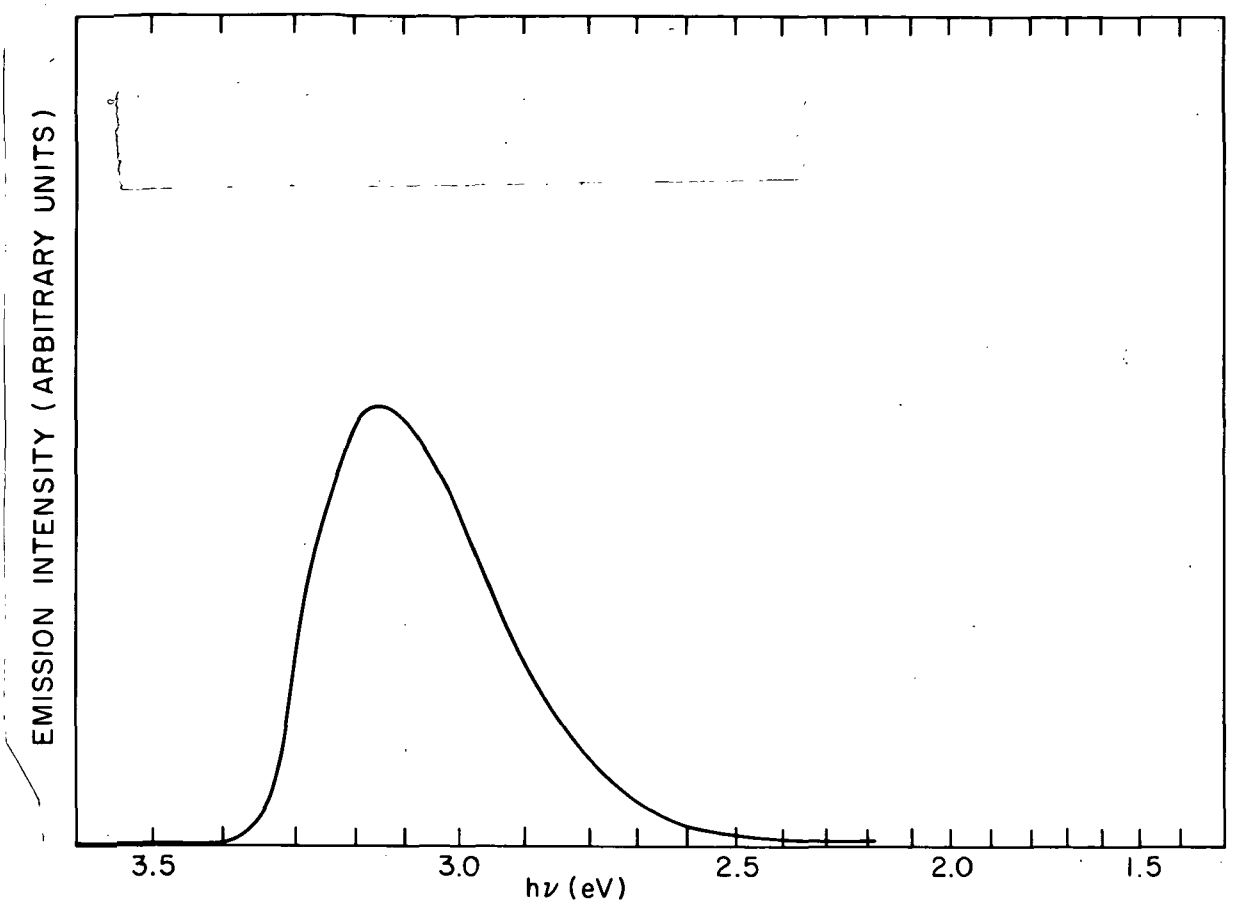

Figure 11. Photoluminescence spectrum of Dy-doped GaN.

F. Carbon

To dope GaN with C, either CH_3 or CN gases were introduced into the reaction tube. C-doping had no noticeable effect on the photoluminescence of GaN, but the electron concentration was raised into the 10^{19} cm^{-3} level.

G. Magnesium

The Mg-doping of GaN has been successfully accomplished by H. P. Maruska at Stanford University (ref. 23). The material becomes insulating and exhibits an efficient photoluminescence at 2.9 eV. We have played a minor part in this effort by contributing some of the early measurements (ref. 24).

H. Lithium

For Li-doping, the GaN was grown by M. T. Duffy of our laboratories using the metal-organic vapor deposition technique of Manasevit et al. (ref. 25). In this method, trimethylgallium is reacted with NH_3 at about 1000°C on a sapphire substrate supported by an rf-heated graphite susceptor. This method is described in greater detail in reference 26. When the resulting GaN is not deliberately doped, an electron concentration of about 10^{19} cm^{-3} is obtained, which is one order of magnitude higher than that obtained by the GaCl method of Maruska and Tietjen (ref. 1). In order to introduce Li, the rf-heated graphite susceptor was impregnated with Li before growing the GaN. The resulting GaN was insulating.

The photoluminescence spectrum of Li-doped GaN is shown in Fig. 12. A peak at 2.23 eV is obtained in addition to the near-edge and the donor-acceptor emission peaks at 3.48 and 3.3 eV, respectively. This spectrum

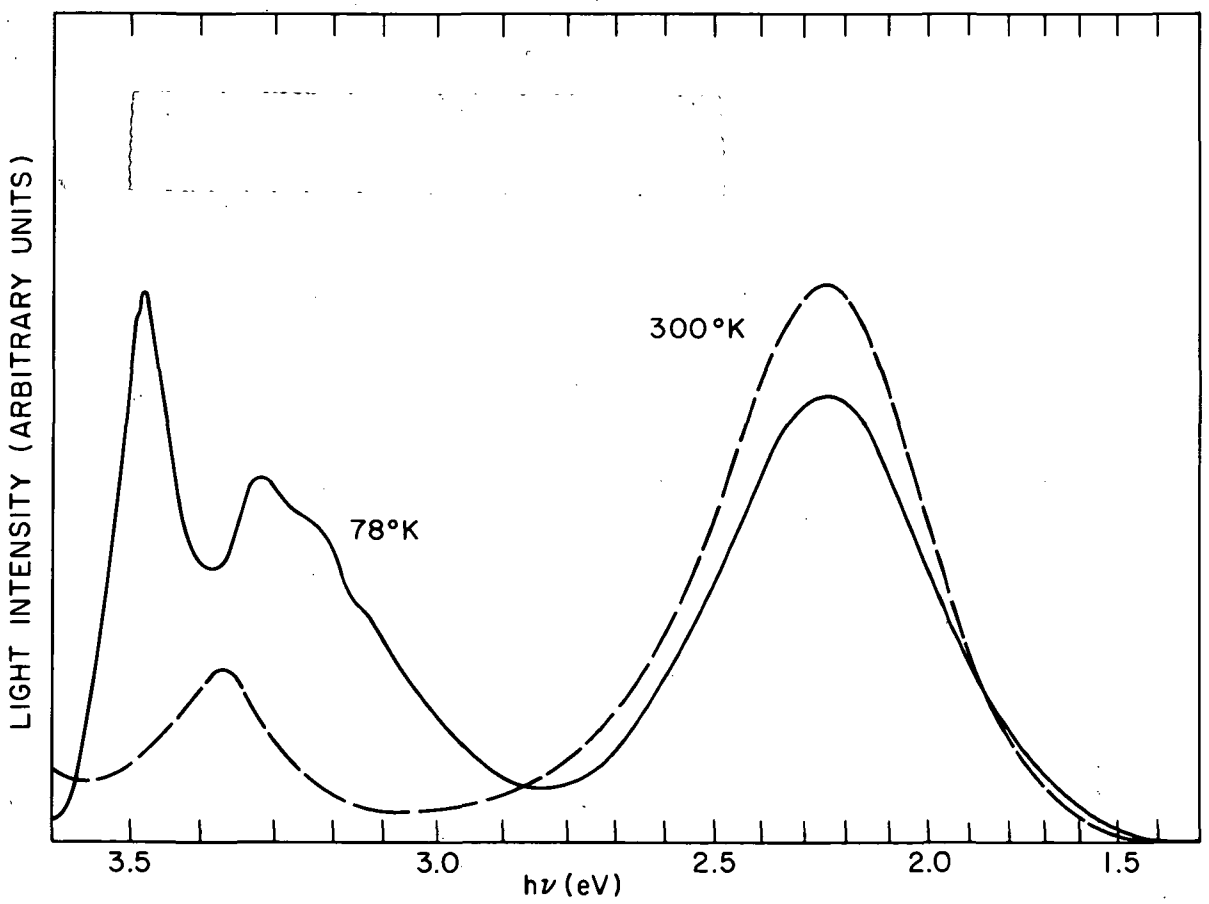

Figure 12. Photoluminescence spectra of Li-doped GaN.

is similar to that obtained by Grimmeiss and Koelmans in powdered or microcrystalline GaN (ref. 27).

I. Zinc

Zn-doping compensates the native donors of GaN and forms a center responsible for efficient blue photoluminescence (ref. 28). Since Zn-doped GaN has been very successful as an electroluminescent material, most of our attention was devoted to the study of this dopant. The following procedure was adopted. First, undoped layers were grown. These had an electron concentration of about 2×10^{18} cm^{-3} and a mobility of about 130 $cm^2/V \cdot sec$. Then, these crystals were cut into two pieces. One of these pieces and a companion virgin sapphire substrate were placed in the reaction chamber. Thus, it was possible to study the electrical and optical properties of the Zn-doped layer grown directly on the sapphire substrate, and also the properties of i-n diodes made with the two-layer GaN.

1. Dependence of Material Properties on Source Temperature. - The temperature of the Zn source was changed from run to run over the range of 280° to 460°C. This corresponds to a partial pressure of Zn in the range 8×10^{-4} to 6×10^{-1} Torr (ref. 22). When GaAs is Zn-doped in this range of partial pressures, the corresponding hole concentration falls in the range 1×10^{16} to 6×10^{18} cm^{-3}, thus providing a calibration curve for the acceptor concentration incorporated in GaAs under similar conditions of growth (ref. 29). However, results obtained with GaAs do not necessarily imply identical Zn concentrations in GaN. The Zn-doped runs lasted two minutes at each Zn-source temperature, T_{Zn}.

The electrical measurements (Table I) show that when the Zn-source temperature (T_{Zn}) is at or above 415°C, an appreciable drop in carrier concentration and mobility is obtained, as expected from partial compensation. Above a 425°C Zn-source temperature, complete compensation is obtained.

The photoluminescent spectra (Table II) of all the Zn-doped specimens (except the material grown at the lowest T_{Zn}) exhibit the blue emission peak at 2.86 ± 0.02 eV. The half width of this band is always about 350 meV. The near-gap emission at about 3.45 eV is observable only in the specimens grown with $T_{Zn} \leq 425$°C. The near-gap peak is the dominant emission for the two lowest Zn dopings, obtained at $T_{Zn} = 280$° and 320°C.

For the photoluminescence measurements made at liquid-nitrogen temperature, the intensity of the blue emission increases with T_{Zn} up

to that temperature for which complete compensation occurs; and beyond this point the luminescence efficiency seems to saturate (Fig. 13a). Measurements made at room temperature, on the other hand, show that the luminescence efficiency is maximum at about T_{Zn} = 415°C, corresponding to growth conditions when substantial compensation occurs (Fig. 13b). At the higher range of T_{Zn}, the apparent drop in room-temperature efficiency reflects the onset of temperature-dependent nonradiative processes, as will be shown next.

2. Temperature Dependence of Photoluminescence. - The photoluminescent efficiency drops rapidly above ∿ 160 K (Fig. 14). The centers responsible for competing nonradiative transitions have a thermal activation energy in the range of 0.44 to 0.19 eV for specimens grown in the T_{Zn} range of 410° to 450°C (only a few specimens were tested). These values of activation energy for the nonradiative recombination are consistent with those obtained by Ilegems et al. (ref. 21) in very lightly doped GaN.

The emission peak of the material used to obtain Fig. 14 occurs at 2.85 ± 0.01 eV over the temperature range 78 to 286 K, confirming the findings of Grimmeiss et al. (ref. 28) and of Ilegems et al. (ref. 21) that this peak does not shift substantially with temperature. This temperature independence contrasts with the change, of the order of 100 meV, for the energy gap over this temperature range. The markedly different spectral behavior of the 2.85-eV emission line and of the energy gap is an empirical indication that the Zn center may be associated with a vacancy (ref. 30).

3. Dependence of Photoluminescence on Excitation Intensity. - The photoluminescence of several Zn-doped layers was measured at 78 K as a function of the intensity of the UV excitation. A set of calibrated filters was used to attenuate the incident radiation from a UV laser. Figure 15 shows that the output is nearly proportional to the input over about 4 orders of magnitude (the maximum level of excitation in this case being about 3 mW). The emission peak shifts to higher photon energies with increasing excitation (Fig. 16). This plot suggests an exponential dependence $L \propto \exp \frac{h\nu}{E_o}$ ($E_o \approx 5$ meV) which would be expected from an exponential distribution of states either in the conduction band or in the impurity band (or in both). A 5-meV tailing coefficient in another compound, GaAs, is commonly found in lightly doped materials (ref. 31). Hence, the GaN used in Fig. 16 (grown with T_{Zn} = 425°C) does not appear to be seriously strained or strongly doped, at least not near the surface.

TABLE II

Photoluminescence Data at 78 K for Zn-doped GaN

T_{Zn} (°C)	hν (eV)	Δhν (meV)	Other Peaks at (eV)
280			3.44
320	2.88		3.45,3.33
360	2.87	350	3.44
380	2.87	350	3.45
390	2.87	350	3.45
400	2.88	350	3.45,3.33
405	2.87	350	3.45,3.33
410	2.87	350	3.45,3.33
415	2.86	350	3.45,3.33
420	2.86	350	3.45
425	2.86	350	3.45
430	2.87	350	
435	2.85	350	
440	2.87	350	
445	2.87	350	
450	2.86	350	
455	2.87	350	
460	2.87	360	

TABLE I

Electron Concentration and Mobility in Zn-doped GaN

T_{Zn} (°C)	N_e (cm^{-3})	μ_e ($cm^2/V \cdot sec$)
280	3.3×10^{18}	136
320	4.5	142
360	1.7	62
380	2.5	112
390	1.0	94
395	2.4	86
400	1.3	82
405	7.8	80
410	1.2	106
415	0.1	76
420	0.9	73
420	0.7	15
425	0	0

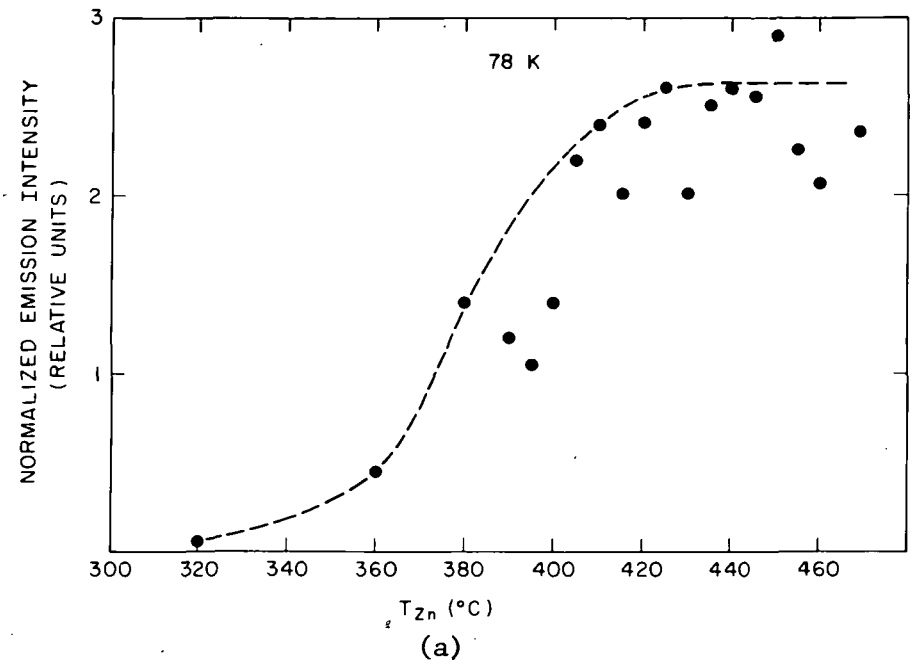

(a)

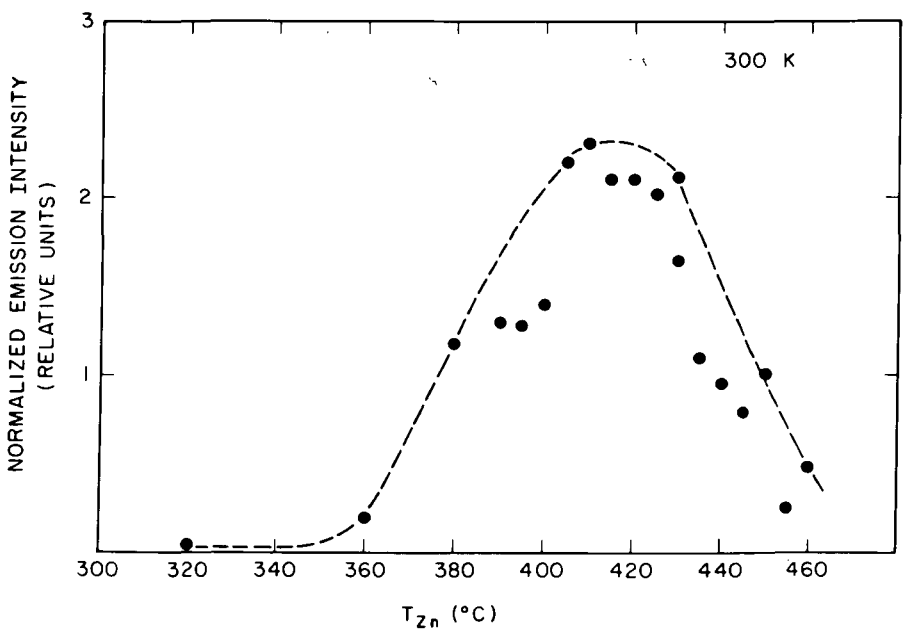

(b)

Figure 13. Dependence of photoluminescence intensity on the temperature T_{Zn} of the Zn-source. (a) Data obtained at 78 K, (b) data obtained at 300 K.

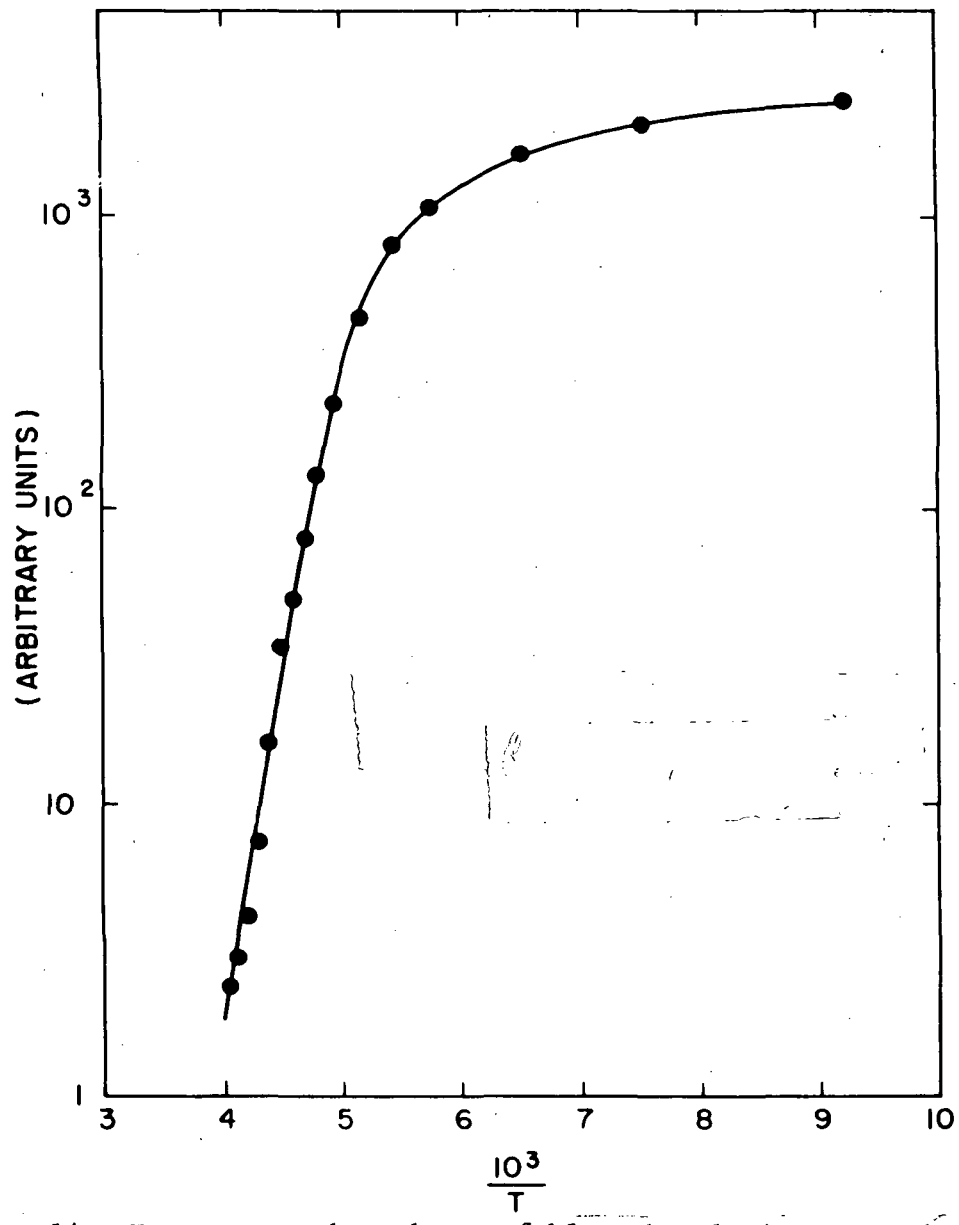

Figure 14. Temperature dependence of blue photoluminescence in Zn-doped GaN.

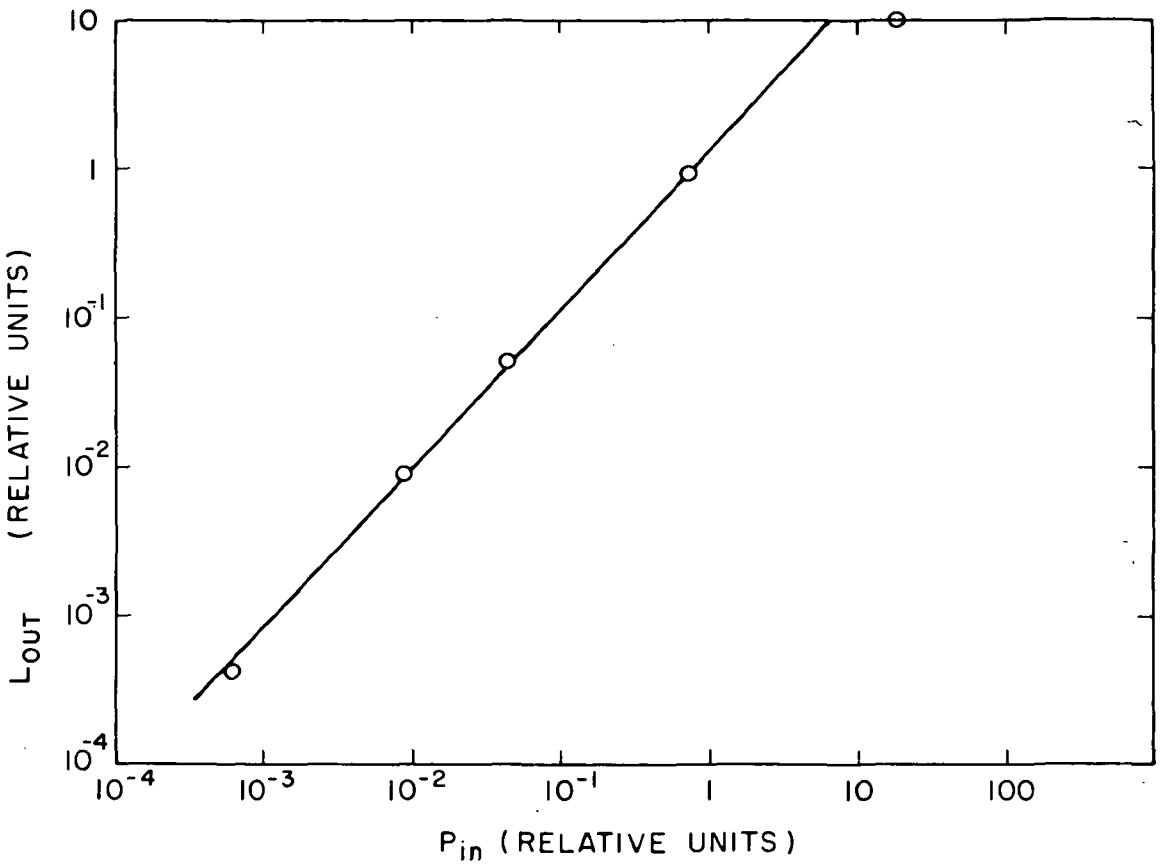

Figure 15. Dependence of emission intensity as a function of optical excitation.

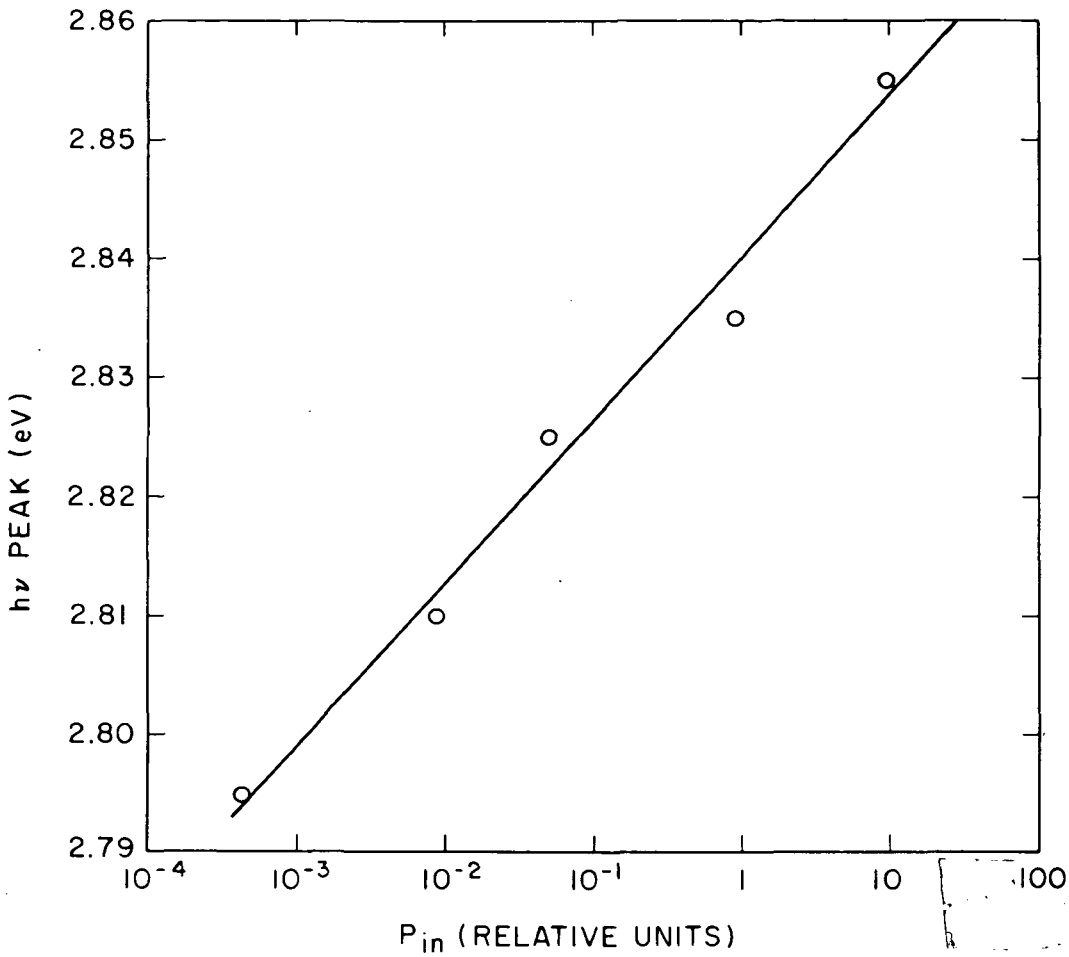

Figure 16. Spectral shift as a function of excitation intensity.

4. Effect of Growth Temperature on the Properties of Zn-doped GaN. - A series of crystals were grown at different temperatures on a blank sapphire substrate and on a previously grown undoped n-type crystal. Each crystal was grown for 5 minutes. The growth temperature started at 960°C and was dropped initially in 20° steps until 760°C; a final run was made at 700°C. The partial pressure of Zn was maintained constant during all these runs by maintaining T_{Zn} at 425°C. All of the crystals grown on blank sapphire substrates were insulating.

The photoluminescent efficiency was measured at 78 K. The result, plotted in Fig. 17, shows that the efficiency is nearly independent of the growth temperature above 850°C. However, there is a rapid drop in efficiency for crystals grown at the lower temperatures.

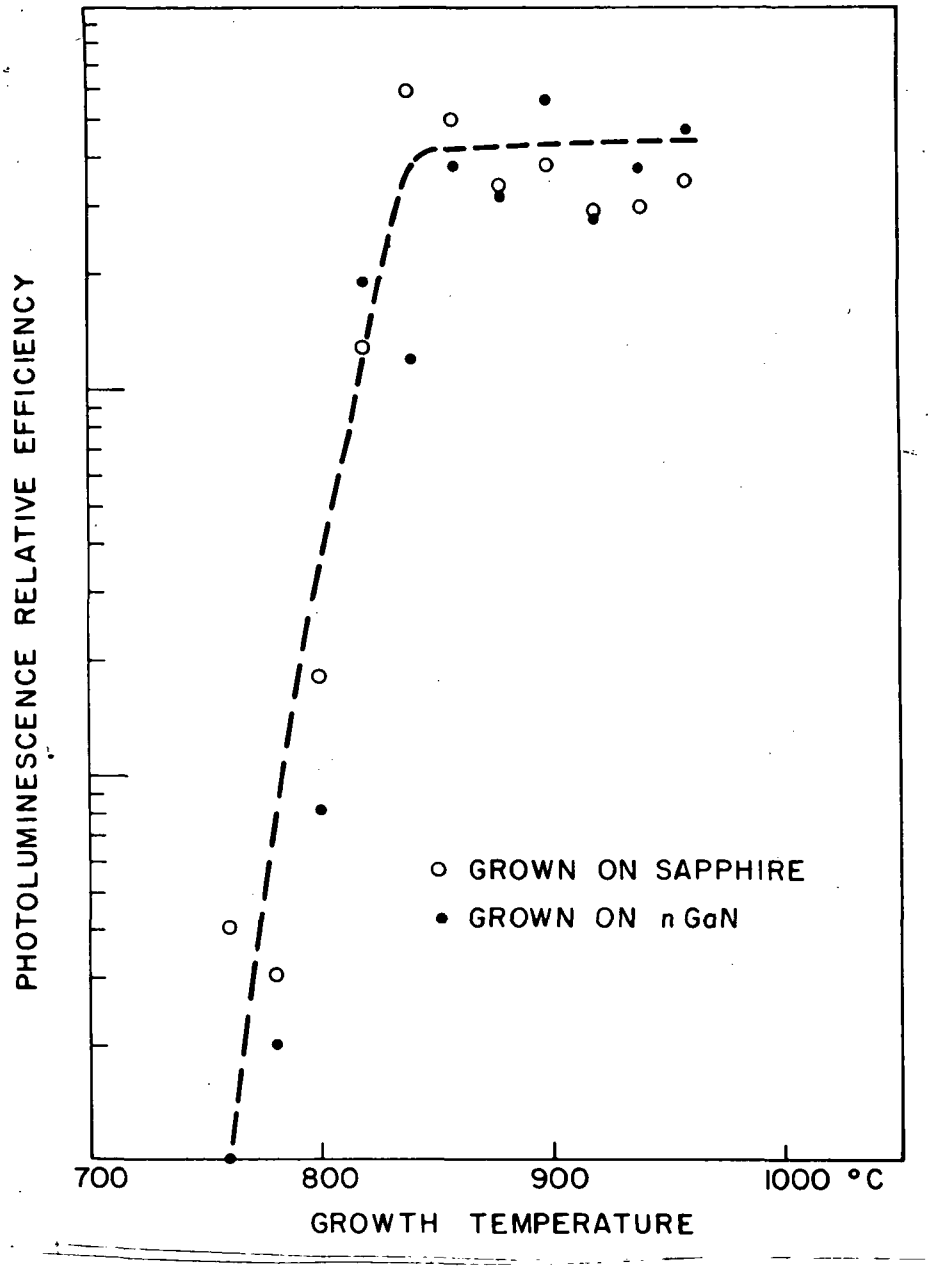

Figure 17. Dependence of photoluminescence efficiency on the temperature at which the Zn-doped GaN was grown.

For material grown below 800°C, the spectral dependence is very pronounced (Fig. 18), starting from red and rapidly reaching blue. Growth temperature between 800° and 960°C has very little effect on the emission spectrum which shifts slightly to higher photon energies with increasing growth temperature.

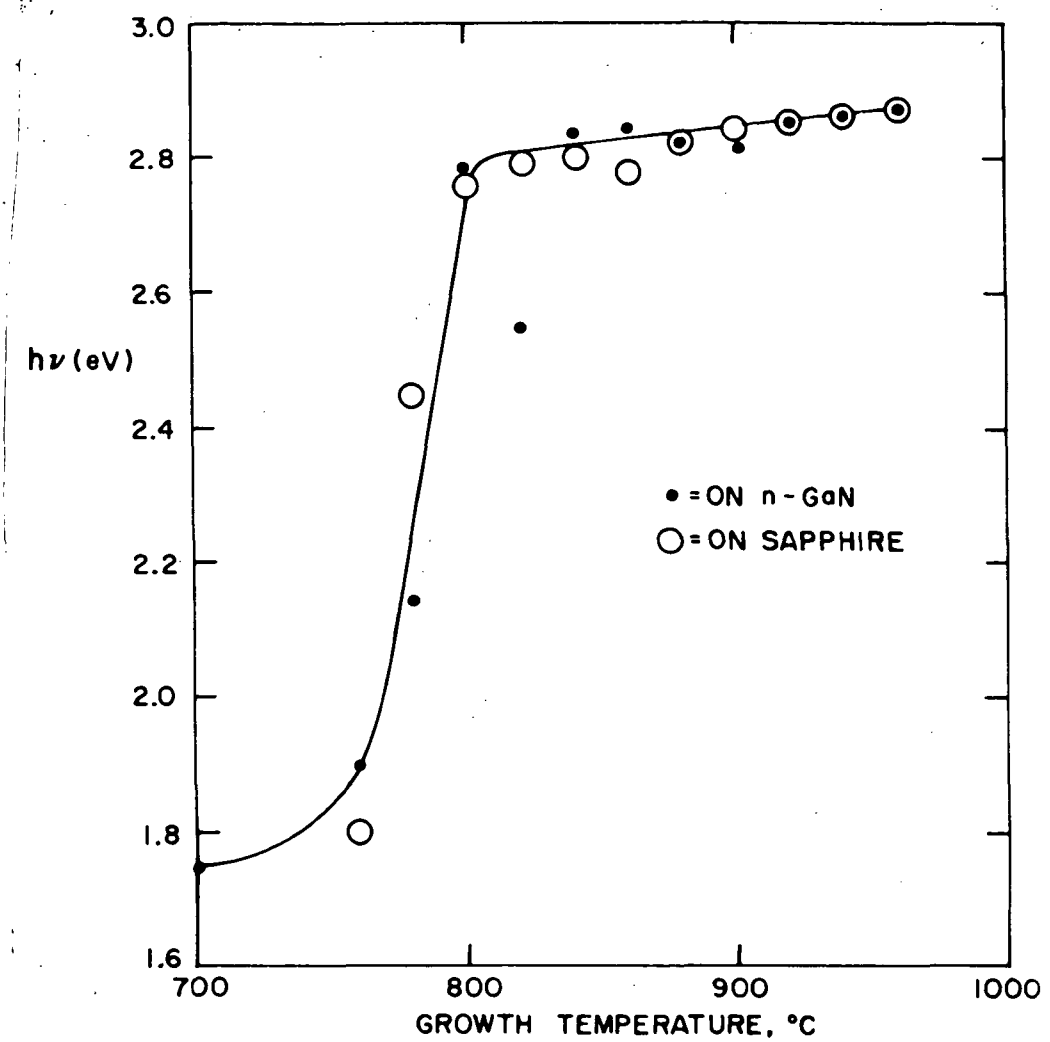

Figure 18. Effect of the growth temperature on the position of fluorescence peak of Zn-doped GaN.

5. Effect of Growth Duration on the Properties of Zn-doped GaN. - As the crystal grows, the interfacial stress is gradually relieved. Such stress relief must affect the ability to incorporate Zn and the efficiency of the radiative process.

Several Zn-doped layers were grown at 950°C (T_{Zn} = 448°C) for durations ranging from 10 sec. to 20 min.

At room temperature, there is no correlation between the emission spectra and the growth duration, t. However, at 78 K, as t increases, the emission peak shifts to lower energies while the linewidth broadens (Fig. 19). The photoluminescence efficiency goes through a maximum

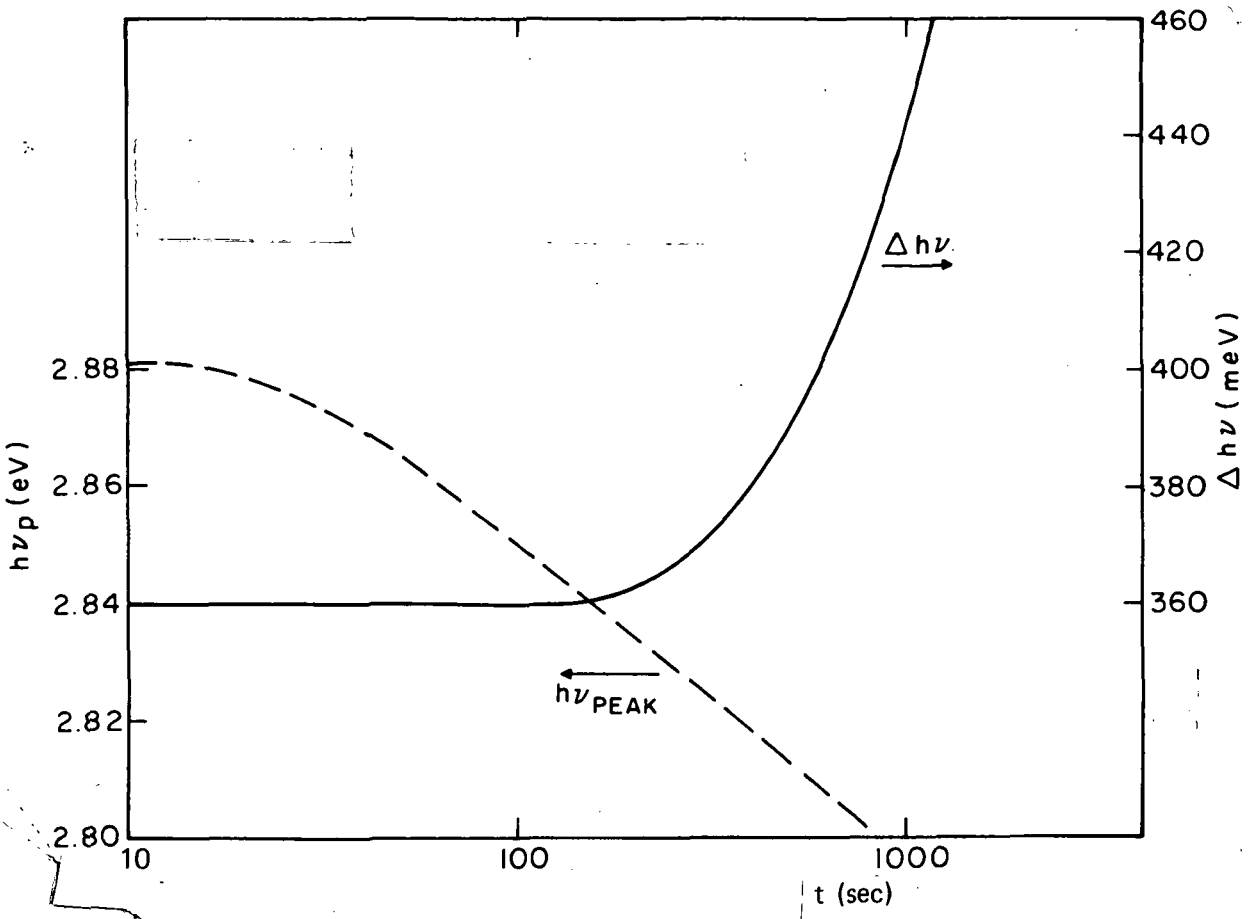

Figure 19. Dependence of emission peak and linewidth on growth duration of Zn-doped GaN.

when the growth duration is one minute (Fig. 20). The lower efficiency of thinner layers may be due to the presence of interfacial strains which could cause a dominance of nonradiative recombination. As the crystal grows thicker, the stresses decrease and more Zn is accommodated into the lattice. The presumed increase in Zn concentration is consistent with the spectral broadening and shift to lower photon energies.

The data obtainable at 2 min. growth-time is compatible with the data presented earlier, when T_{Zn} was the parameter varied between two minute growths.

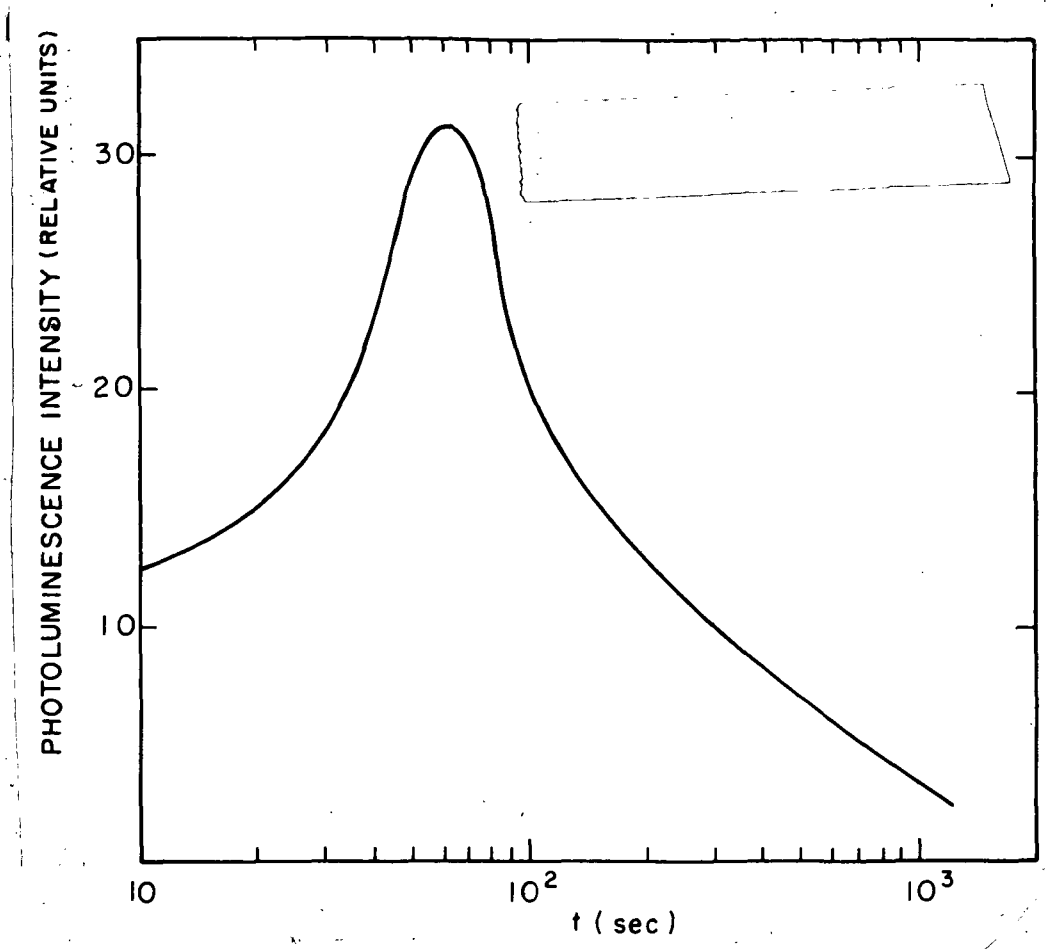

Figure 20. Dependence of emission efficiency on growth duration of Zn-doped GaN.

V. ION IMPLANTATION

Ion implantation permits the introduction of a known concentration of an isotopically pure elemental impurity into a thin layer at the surface of the crystal.

One drawback of implantation is the tremendous damage induced in the crystal independently of the element used. The implanted region is visibly darker than the unimplanted region and exhibits highly insulating properties -- probably because of very low carrier mobility. However, after annealing, electrical and optical properties are recovered. The annealing treatment is done in an ammonia ambient to prevent decomposition.

Ge^+ was implanted to produce a constant doping profile of 1.0×10^{19} cm^{-3} between 420 and 60 Å from the surface. After annealing, the near-gap photoluminescence peak at 3.4 eV reappeared. Another peak at 2.1 eV was enhanced. However, no structure between 2.0 and 3.5 eV could be found that might be characteristic of Ge. Our earlier work with Ge doping from the vapor phase also did not produce any luminescent peak characteristic of Ge. On the other hand, heavy doping with Ge increases the electron concentration and causes a shift of the Fermi level into the conduction band -- this shows up as a broadening and a shift of the near-gap emission spectrum (ref. 32).

Be^+ implanted into GaN shows, after annealing, a broad peak at 2.16 eV which is characteristic of Be; the same peak is obtained when this element is introduced from the vapor phase.

Mg^+, on the other hand, gives a new photoluminescent peak at 2.34 eV. Mg-doping from the vapor phase always yields only one peak at 2.9 eV (refs. 23, 24).

Ca^+, Dc^+, Ag^+, Sr^+, Li^+, and C^+ were implanted into different areas of the same GaN crystal containing 3×10^{18} electrons/cm^3. The implantation was programed to place 5×10^{18} ions/cm^3 forming a flat profile extending about 400 Å below the surface. After implantation, the crystal was annealed at 1050°C for about 1 hr., and, after annealing, the surface layer appeared conducting. The implantation schedule and the resulting photoluminescence spectra are summarized in Table III.

*This work was done in collaboration with J. A. Hutchby (NASA Langley Research Center).

TABLE III

Ion-Implanted GaN

	Implantation Schedule					Photoluminescence	
Ion	Fluence at Energy	Fluence at Energy	Fluence at Energy	Fluence at Energy		at 78 K	at 300 K
$^{40}Ga^{+}$	1.9×10^{13} 100 keV	6.1×10^{12} 55 keV	4.1×10^{12} 27 keV	2.1×10^{12} 12 keV		3.2, <u>2.48</u>	2.50
$^{114}Cd^{+}$	7.0×10^{12} 100 keV	2.3×10^{12} 60 keV	2.1×10^{12} 35 keV	1.2×10^{12} 20 keV	1.1×10^{12} 11 keV	3.2, <u>2.69</u>	2.70
$^{107}Ag^{+}$	7.2×10^{12} 100 keV	2.4×10^{12} 60. keV	2.1×10^{12} 34 keV	1.2×10^{12} 19 keV	1.0×10^{12} 10 keV	3.2, 2.15, <u>1.50</u>	2.12, <u>1.55</u>
$^{88}Sr^{+}$	9.0×10^{12} 100 keV	3.0×10^{12} 58 keV	2.3×10^{12} 32 keV	1.7×10^{12} 17 keV		3.2, <u>2.16</u>	2.17
$^{7}Li^{+}$	8.5×10^{13} 100 keV	3.3×10^{13} 66 keV	3.8×10^{12} 41 keV	2.8×10^{13} 22 keV		2.15	2.15
$^{12}C^{+}$	5.7×10^{13} 100 keV	2.2×10^{13} 60 keV	1.8×10^{13} 32 keV	9.1×10^{12} 14 keV		2.17	2.15
control	u n d o p e d					<u>3.44</u>, 3.33, 3.24, 2.22, 1.75	<u>3.41</u>, 1.75

Note: Underlined values indicate the dominant peak.

Zn^+ produced the expected peak at 2.87 eV. The efficiency of this peak kept increasing with each annealing step. However, the highest annealing temperature was 1050°C -- from previous experience, some decomposition of GaN is obtained at 1100°C.

To find the effect of doping concentration on photoluminescence, an undoped GaN wafer was mounted behind a metallic mask having an open 60° sector. Thus, six different doses of Zn^+ could be implanted in different regions of the same crystal. The data is tabulated in Table IV, and the resulting spectra are reproduced in Fig. 21.

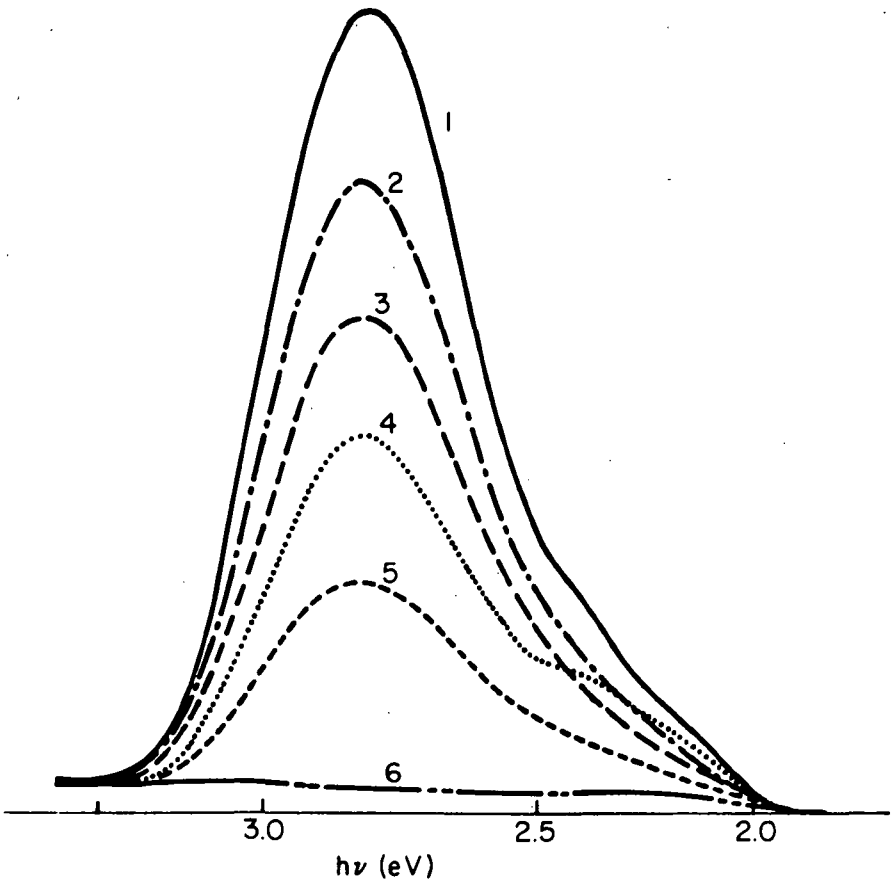

Figure 21. Photoluminescence spectra of GaN Zn-doped by ion implantation. The six curves correspond to different Zn concentrations ranging from (1) 1×10^{18} cm^{-3} to (6) 2×10^{19} cm^{-3} (see Table IV). This data was taken at room temperature.

TABLE IV

Effect of Zn^+ Implantation

Position	Dose in ions/cm^2 at Each Energy				Zn Concentration cm^{-3}
	100 keV	56 keV	29 keV	14 keV	
1	2.4×10^{12}	7.9×10^{11}	5.4×10^{11}	3.5×10^{11}	1×10^{18}
2	4.9×10^{12}	1.6×10^{12}	1.1×10^{12}	6.9×10^{11}	2×10^{18}
3	7.3×10^{12}	2.4×10^{12}	1.6×10^{12}	1.0×10^{12}	3×10^{18}
4	1.2×10^{13}	3.9×10^{12}	2.7×10^{12}	1.7×10^{12}	5×10^{18}
5	1.9×10^{13}	6.3×10^{12}	4.3×10^{12}	2.8×10^{12}	8×10^{18}
6	4.9×10^{13}	1.6×10^{13}	1.1×10^{13}	6.9×10^{12}	2×10^{19}

As with vapor-doped GaN:Zn, the efficiency of photoluminescence at room temperature has a marked dependence on the Zn concentration. This dependence, plotted in Fig. 22, suggests that the photoluminescent efficency is inversely proportional to the logarithm of the Zn concentration or, in other words, that the probability for nonradiative transition increases with the logarithm of the impurity concentration.

For the purpose of associating the emission spectrum with a given impurity, it is not evident that the distribution profile need be constant near the surface. A special experiment, using Zn^+, was designed to answer this question. A GaN wafer containing 3×10^{18} electrons/cm^3 was implanted over one region with 100-keV Zn^+ and over another region with fluences and energies designed to produce a flat profile of 5×10^{18} Zn/cm^3. The information schedule is shown in Table V.

After annealing for 1 hr. at 1000°C in ammonia, both regions produced identical photoluminescent spectra peaking at 2.88 eV. Hence, for the purpose of spectroscopic impurity identification, the implantation profile is not critical.

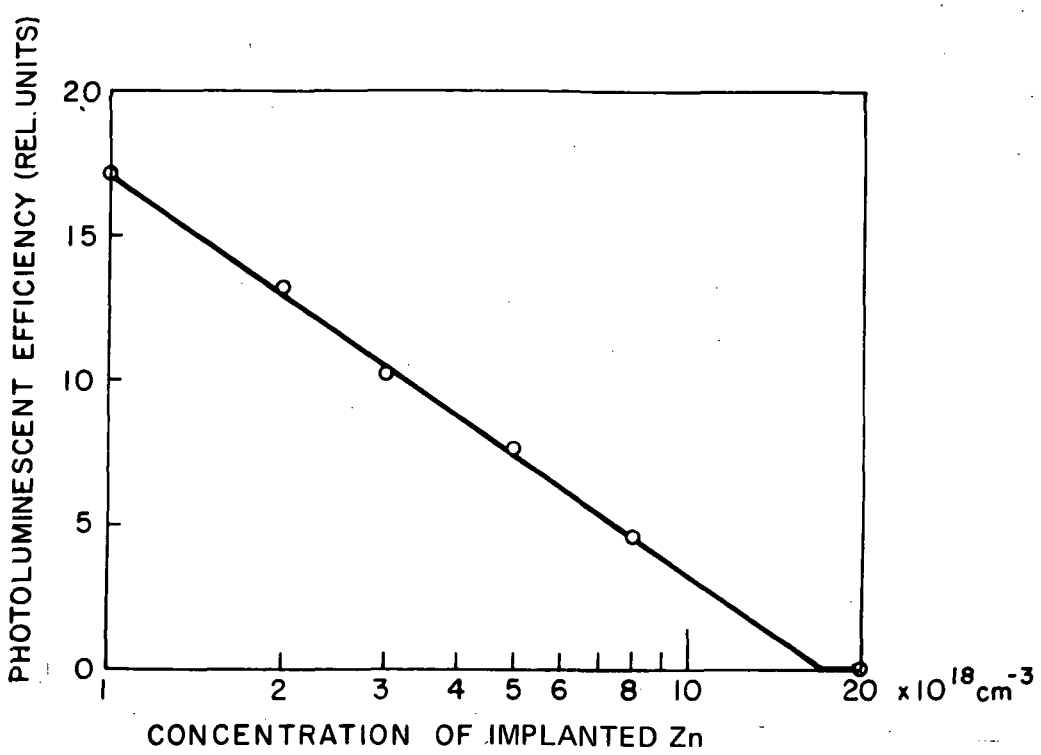

Figure 22. Dependence of the photoluminescence efficiency at room temperature on the concentration of implanted Zn.

TABLE V

Zn Implantation Schedule

Position	Fluence at Tabulated Energy			
	100 keV	56 keV	29 keV	14 keV
1	1.2×10^{13}	3.9×10^{12}	2.7×10^{12}	1.7×10^{12}
2	1.3×10^{13}	0	0	0

VI. GaN LIGHT-EMITTING DIODES

A. M-i-n Diode Fabrication

The electroluminescence of GaN has been studied using the structure illustrated in Fig. 23. First, an undoped n-type conducting layer is grown on sapphire. Then a thin Zn-doped insulating layer is grown on the n-type layer. The wafer is cut into 1-mm-diameter discs or squares which are then soldered with indium to a ceramic support. This peripheral solder makes an ohmic connection to the n-type layer. A small indium dot soldered at the center of the insulating layer forms a 10^{-3}-cm^2 area of nonohmic connection.

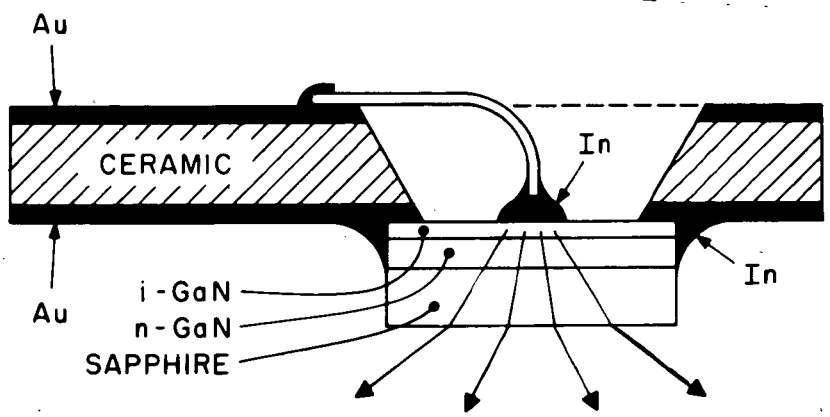

Figure 23. Structure of the GaN LED.

B. LED Performance

When current is passed through the diode, light is emitted in the insulating layer. This process can occur with either polarity of bias, generating cw light at room temperature. The luminescence mechanism is discussed later.

1. Electrical Characteristics. - The I-V characteristic of the diode exhibits a power dependence: $I \propto V^n$, where n can be in the range of 3 to 6 at low currents (less than about 10^{-5} A), becoming approximately 2 at higher currents. The quadratic dependence of the I-V characteristics (Fig. 24) is suggestive of transport by single-carrier charge-limited current in the presence of traps (33). The dependence of current on voltage becomes stronger when the electric power input is of the order of 0.5 W, causing the diode to become warm. Light is emitted mostly over the quadratic portion of the I-V characteristic, and the emission

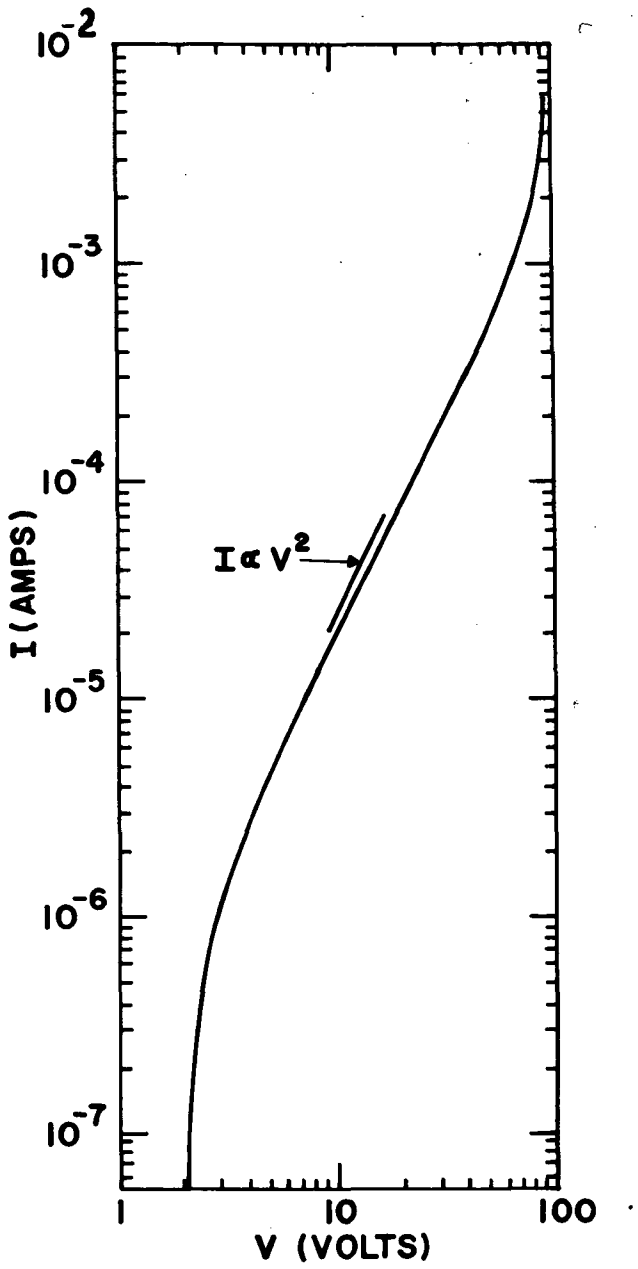

Figure 24. I-V characteristic of GaN LED.

continues at the higher bias where heating occurs. The I-V characteristic of the most efficient unit is shown in Fig. 25, the light being emitted beyond the knee of the curve at about 10 V.

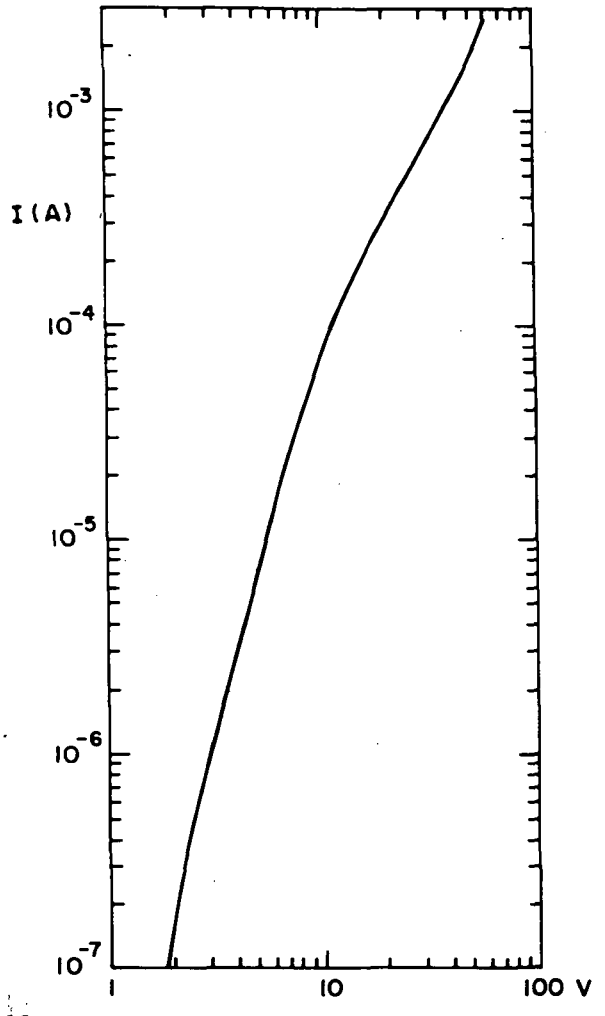

Figure 25. I-V characteristic of M-i-n diode using Zn-doped GaN.

2. Emission Spectrum. - The electroluminescent emission spectrum falls in the visible range. Various examples of spectra obtained were shown in Fig. 4. The spectral position of the emission peak is determined by growth conditions, such as the Zn vapor pressure during growth, the rate of growth, and the duration of the growth. The spectral width at half maximum is at least 350 meV. As the current through the diode is increased, the emission intensity grows, but does not shift in position. In some diodes, the shape and position of the emission spectrum depend on the polarity of the bias. Thus, blue light is emitted when the indium dot is biased negatively; green and yellow light can be generated with either polarity; red is usually found only with a negative bias in diodes which, with a positive bias, emit either yellow or

green light. For our brightest diode, the emission spectrum peaks at 2.39 eV (5190 Å) and has a linewidth of 0.41 eV (Fig. 26).

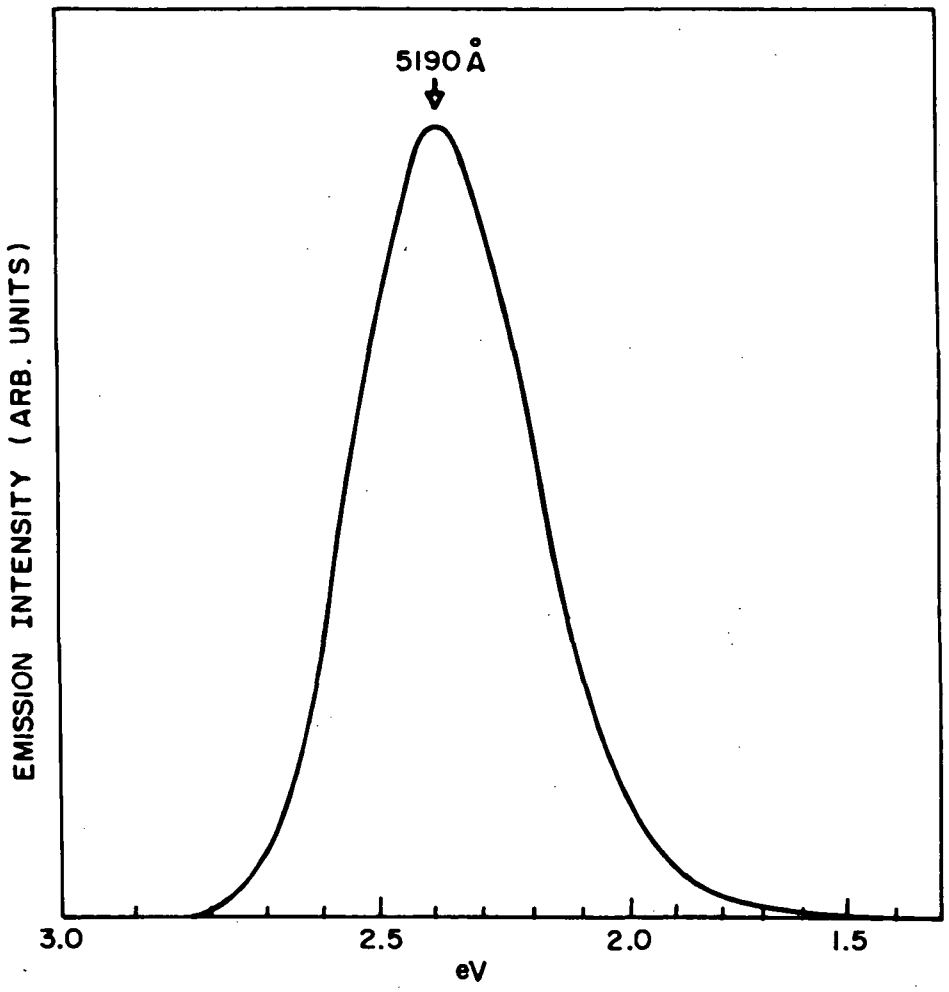

Figure 26. Emission spectrum of GaN LED of Fig. 25.

3. Efficiency. - The radiated power is usually proportional to the electric power input, but tends to saturate when the power input exceeds 0.5 W. If, however, the diode is pulsed, the linear dependence of power output on driving power can be extended by about one order of magnitude. For our best diode, the light output rises rapidly at first, and then becomes nearly linear with the input power (Fig. 27). From the latter data one can see that the power efficiency is about 0.1%.

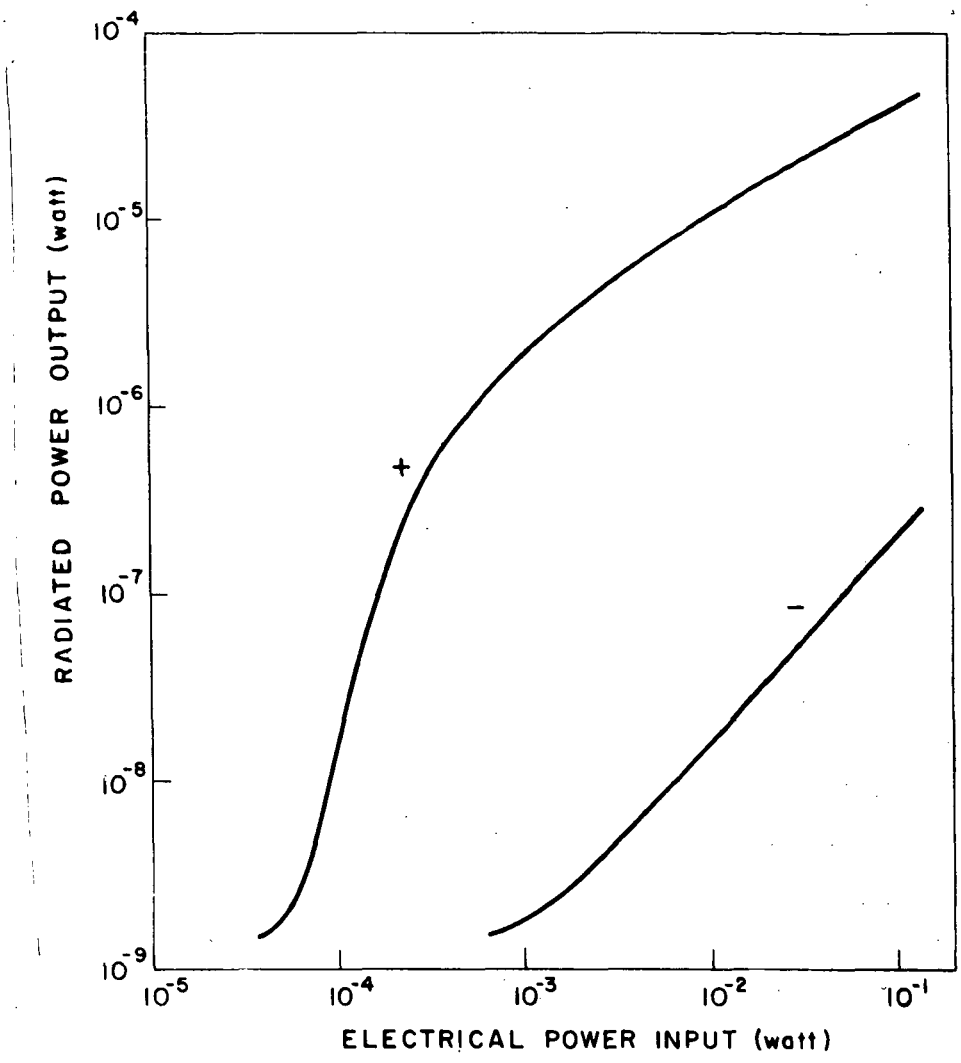

Figure 27. Radiated power output at 5190 Å vs. electrical power input for GaN LED. The +- signs refer to the polarity of the metal electrode.

External power efficiencies of 10^{-3} have been obtained several times, with yellow as well as green light-emitting diodes; however, power efficiencies in the range 10^{-4} to 10^{-5} are more common.

The brightness or luminance of a diode having a circular luminous spot 400 μm in diameter measured 300 fL (10^3 Cd/m^2) at a current level of 2 mA and an applied voltage of 50 V. Another diode had a luminance of 850 fL at 600 μA and 22.5 V.

4. Life. - One of our better diodes was subjected to a life test under a continuously applied dc bias of 32 mW. The output showed no evidence of degradation over a period of more than 5 months (Fig. 28).

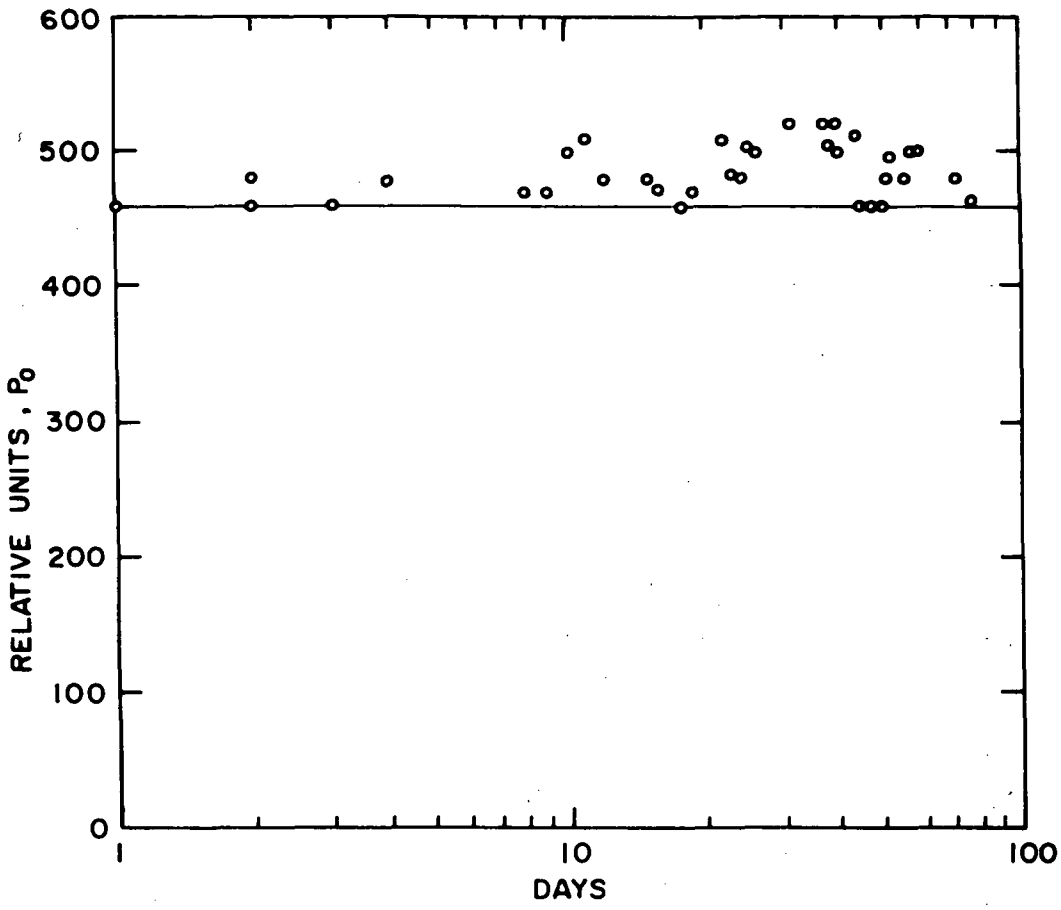

Figure 28. Life test data for GaN LED. The instability is attributed to a noisy contact.

5. Luminescence Delay. - A delay has been found between the onset of electroluminescence and the application of a step excitation (Fig. 29). This delay is tentatively attributed to the emptying of deep traps. The delay of the luminescence has an inverse dependence on the current but not a linear one (Fig. 30). Hence, it is difficult to evaluate an average trap density. With a negative bias, on the other hand, a much shorter delay is observed (Fig. 31b).

If a short probing pulse is superimposed on the excitation pulse, one can explore the status of the traps at various times during the excitation. This is shown in Fig. 32. The bright trace of Fig. 32(b)

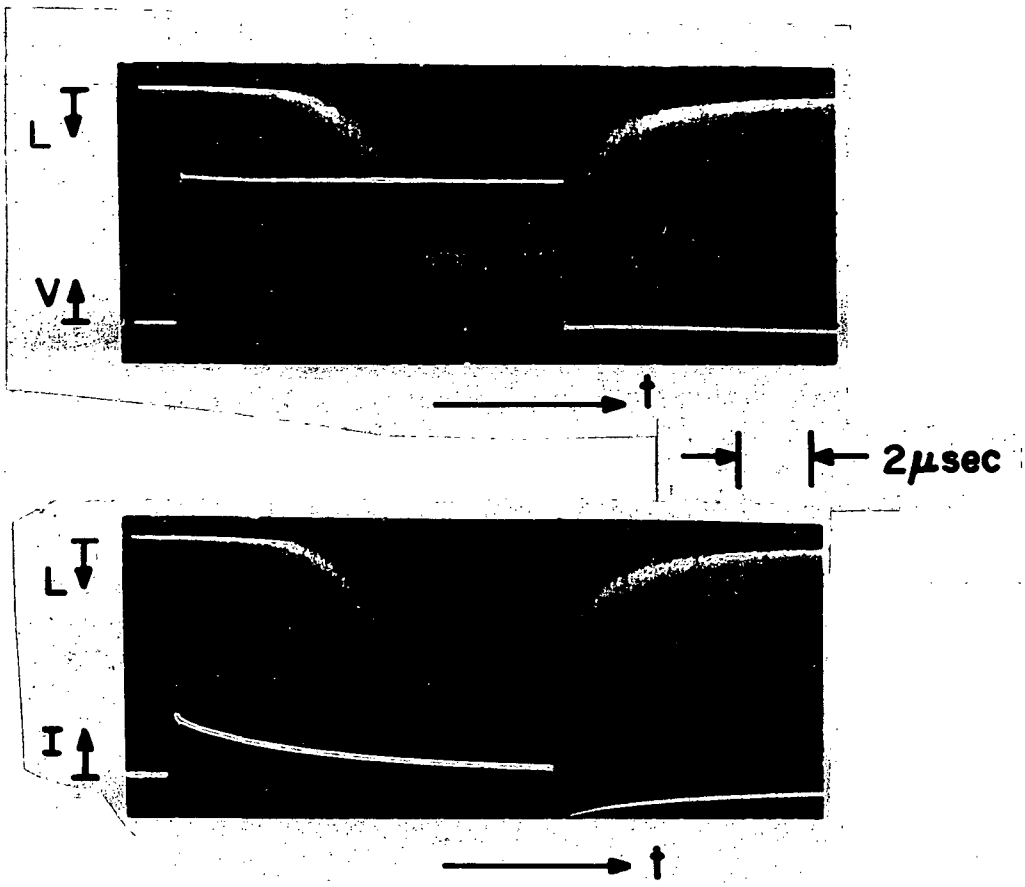

Figure 29. Oscillogram of electroluminescence under pulse excitation.

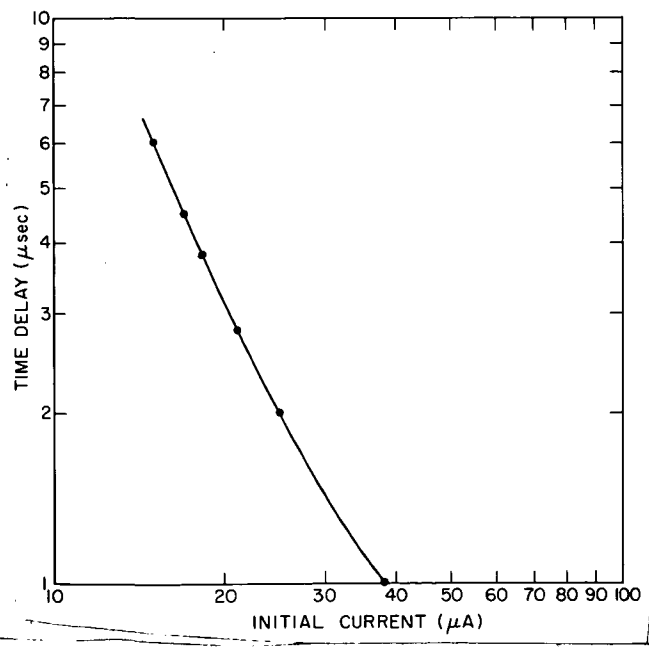

Figure 30. Time delay for a fixed value of light signal (5 times larger than noise) as a function of the initial current during a step excitation.

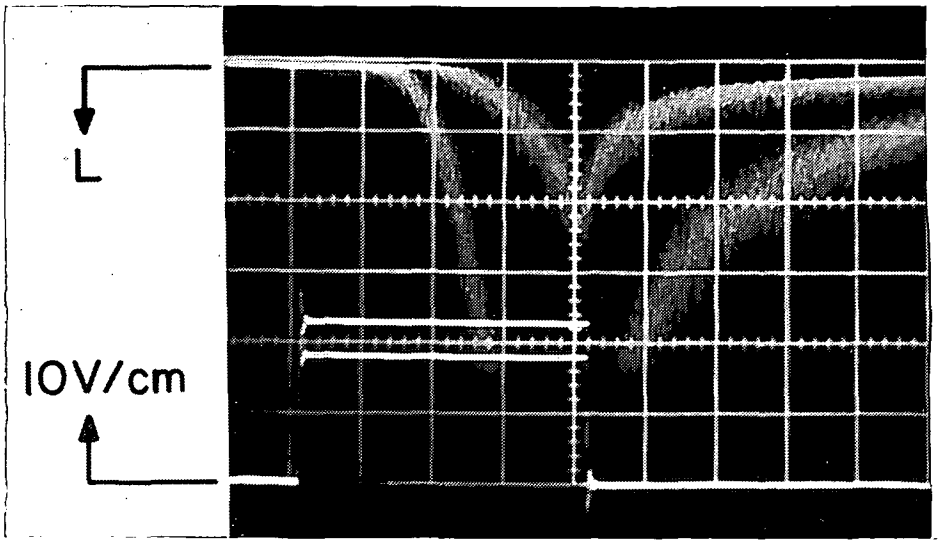

(a)

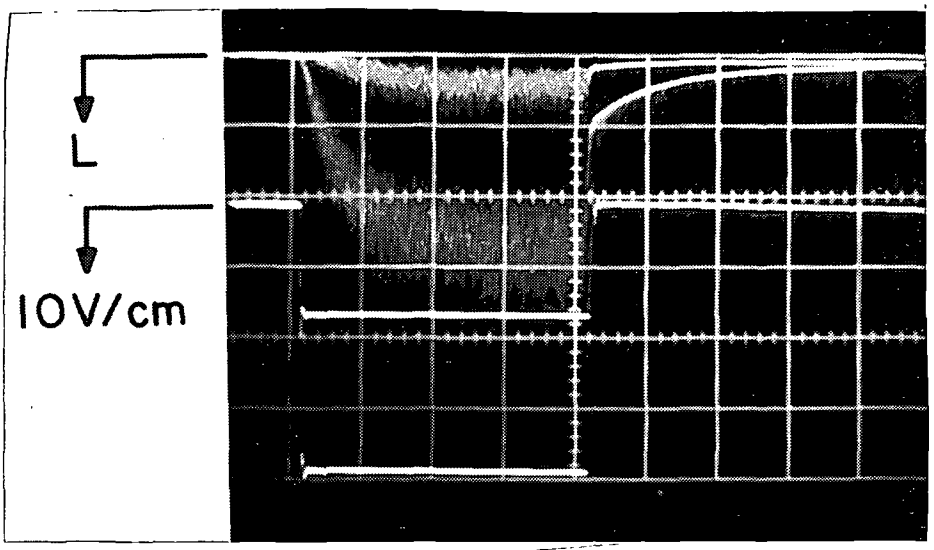

(b)

1 μsec/cm

Figure 31. Oscillograms of electroluminescence under pulsed condition for two values of excitation for each of: (a) positive bias on M; and (b) negative bias on M.

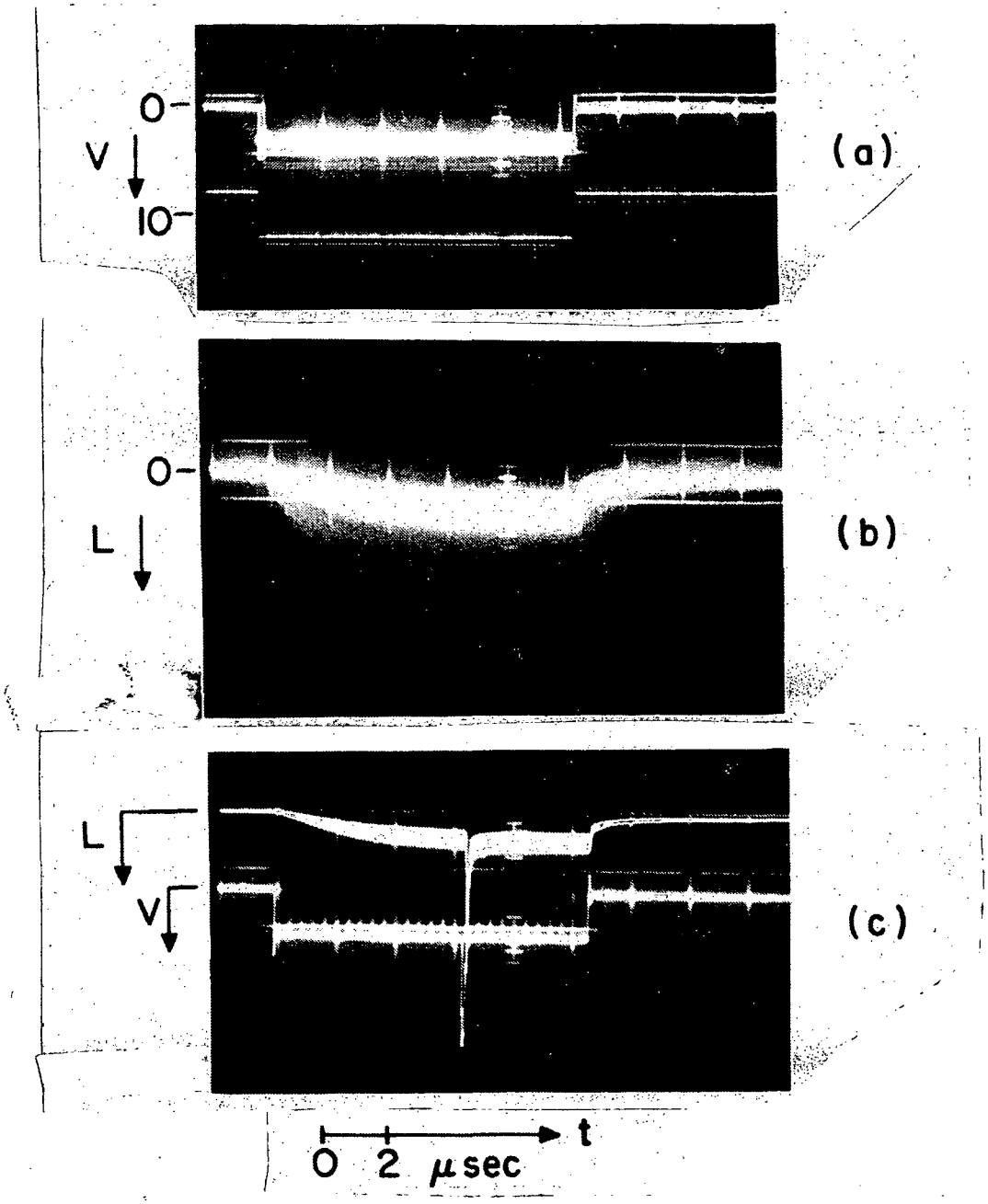

Figure 32. (a) Time dependence of applied voltage pulse. The gray region is produced by the probing pulse which sweeps along the time axis. (b) Time dependence of luminescence in response to the above excitation. The gray region is produced by the sweeping probing pulse. (c) Wave shape of excitation and light output with probing pulse stationary at a time when all the traps have been filled.

shows the intensity of luminescence during the excitation. At this current level, the delay is negligible compared with the time scale used. However, note that the luminescence continues to rise gradually as additional traps are emptied. The evolution of trap emptying is stabilized after 4 μsec, whereupon the emission intensity remains constant. We shall call this condition the "steady state." The envelope of the dimmer region of Fig. 32(b) is the luminescence intensity during the short (100 nsec) probing pulse which scans along the excitation pulse from frame to frame in this multiple exposure picture. The increment of luminescence during the probing pulse grows with the availability of empty traps. Furthermore, the response to the probing pulse is fastest during "steady state." When the excitation is turned off, the luminescence decays in a time of the order of 1 μsec.

6. Frequency Response. - The metal-insulator-semiconductor structure forms a capacitance of the order of 10^{-11} F. Hence, although the recombination process in GaN is very fast (less than 10 nsec), the high-frequency performance of the diode is expected to be limited by its RC time constant.

The resistance involved in determining the rise time of the diode is the lateral internal resistance of the n-type layer between the region under the indium dot and the peripheral ohmic contact. This resistance is estimated to be of the order of 1 ohm. Hence, the frequency response is not expected to be limited by the rise time. However, as we have seen in the previous section, a delay in luminescence could limit the frequency response. On the other hand, if the diode is biased into the steady state condition, a fast response should be obtained.

The decay time, however, is determined by the shunting resistance across the insulating layer. Note that the insulating layer may be inhomogeneous and comprise microscopic conducting inclusions which transform the insulating layer into a random network of capacitors and resistors in complex series and parallel combinations. In this case, both rise and fall times would be determined by the R and C network inside the insulating layer.

The I-V characteristic is nonlinear; therefore, the resistance varies with the bias. Although light emission begins at a bias corresponding to a shunt resistance of 10^5 to 10^6 ohms, at higher currents, the internal resistance can drop by two or three orders of magnitude. Hence, to operate the diode at high frequencies, a dc bias is used to place the diode in a low dynamic resistance range and into the steady state conditon to avoid the delay effect.

Figure 33 shows the response of the diode to a 40-mA pulse superimposed on a 60-mA, 12-V dc bias. The instrumental limitation to the

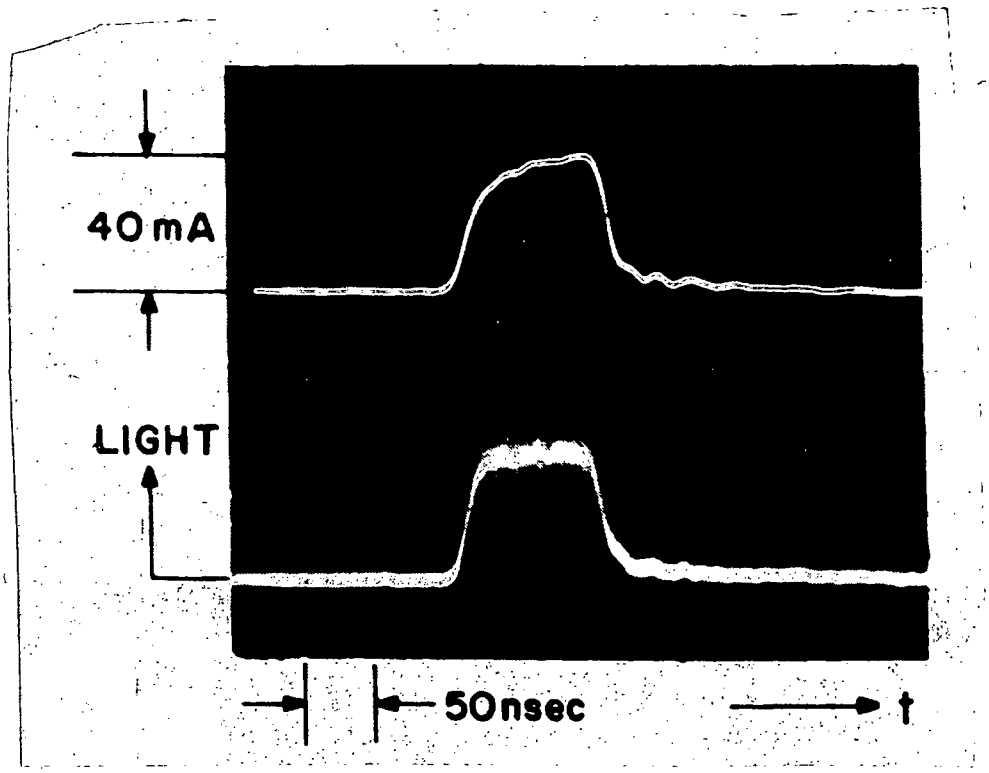

Figure 33. Response of GaN diode to a 40-mA pulse (upper trace) superimposed on a 60 mA 12 V dc bias. The lower trace is the output of the photomultiplier.

response time imposed by the pulse generator is 10 nsec. The rise and fall times are about 15 nsec. Without a dc bias, a decay time constant of the order of 1 μsec was obtained.

Next, a high-frequency generator driving the diode with about 0.5 V was used to superimpose its output on the dc bias of the diode. The output of the photomultiplier was fed into a spectrum analyzer which was used as a tunable receiver and permitted to measure the amplitude of the light signal. The output was flat up to 50 MHz. As shown in Fig. 34, a sharp resonance was observed at 65 MHz before an abrupt cutoff at 75 MHz. We have no explanation for the observed resonance.

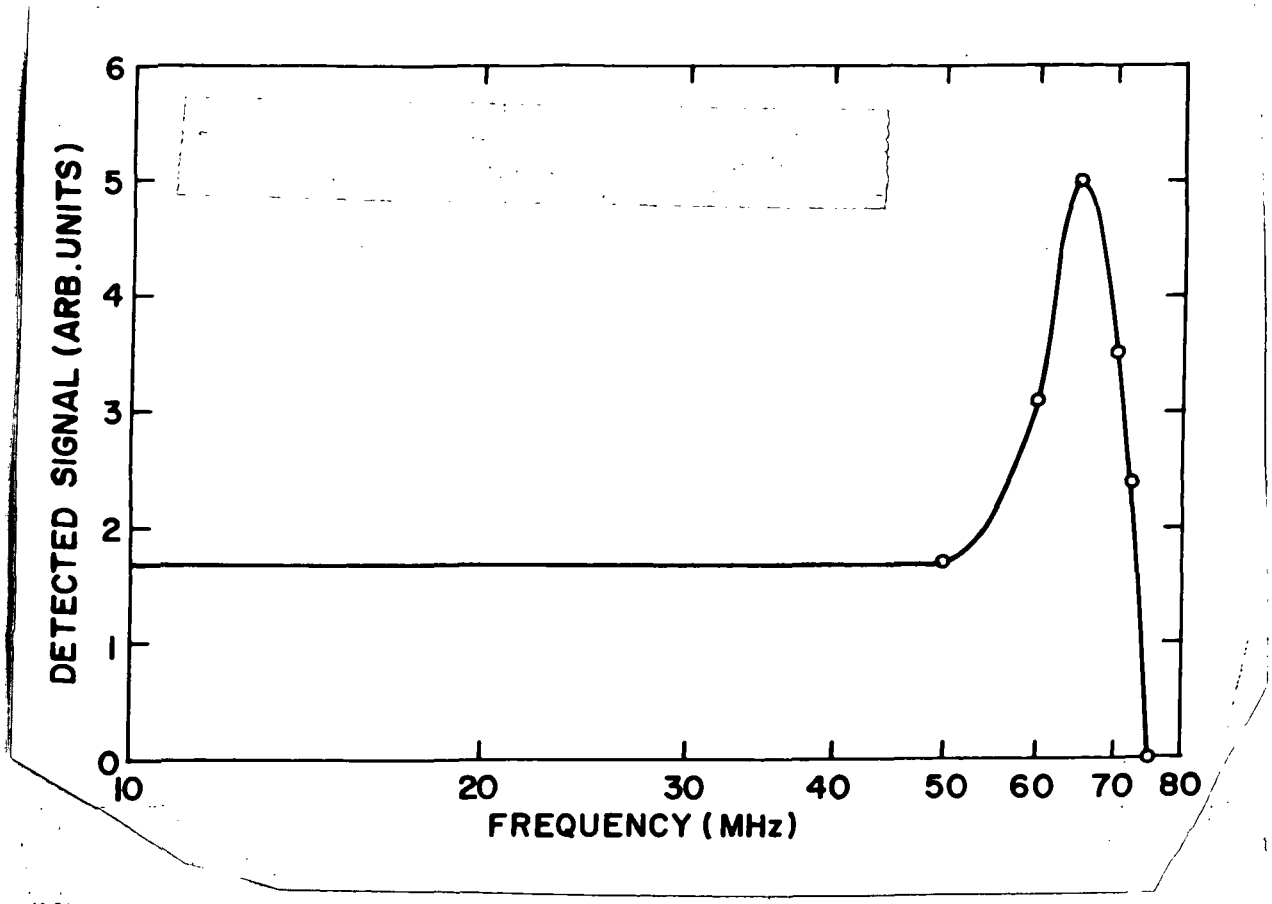

Figure 34. Frequency dependence of the light output from a GaN diode.

VII. MODEL FOR ELECTROLUMINESCENCE IN GaN

Here we shall be concerned with a model for the electroluminescence mechanism operant in the GaN M-i-n diode. Let us first review the most pertinent facts:

1. Light is emitted with both polarities of bias.
2. Emission occurs in the i-region at the cathode.
3. The emission spectrum does not shift or broaden with increasing current.
4. There is a current-dependent luminescence delay with positive bias on M.
5. There is no luminescence delay with a negative bias on M.
6. The I-V characteristic first rises rapidly, then I varies approximately as V^2.
7. A similar, though not identical, I-V characteristic is obtained with either polarity of bias.
8. Light is emitted over the range of quadratic I-V dependence.

Clearly, the luminescence process and the useful charge transport must occur inside the insulating layer. However, the voltage for the onset of electroluminescence does not seem to depend on the thickness of the i-layer. Further, in diodes where a very thick i-layer is used, one can rely on the depth resolution of a stereoscopic microscope to verify where the light originates: when the In dot is negative, the light is emitted at the M-i interface; when the polarity is reversed, the light is generated at the i-n interface; i.e., the light is always generated at the cathode. These two observations, that the light is produced at the cathode and that the voltage for the onset of electroluminescence is independent of the insulator's thickness, suggest that the high field region extends over a short distance from the cathode.

The following model is proposed to explain these observations. At the operating bias which is applied across the insulating layer, field emission transfers electrons from the deep acceptors to the conduction band. This field emission may be enhanced by inhomogeneities in the insulating region, such as a plurality of sharp points. The numerous corners formed by the edges of the growing crystalline facets (Fig. 35) could well act as these sharp points. The smallest resolvable steps between facets in Fig. 35 measure about 200 Å. Hence, both the M electrode and the n-type layer form conducting sharp points capable of generating high local fields in the i-layer. The electrons drifting toward the anode increase the conductivity of the insulating region near the anode, thus reducing the potential drop over part of the i-layer and concentrating the electric field near the cathode as shown in Fig. 36. Hence, the steady state condition would consist of a high field near the cathode and a relatively low field over the rest of the nominally insulating region.

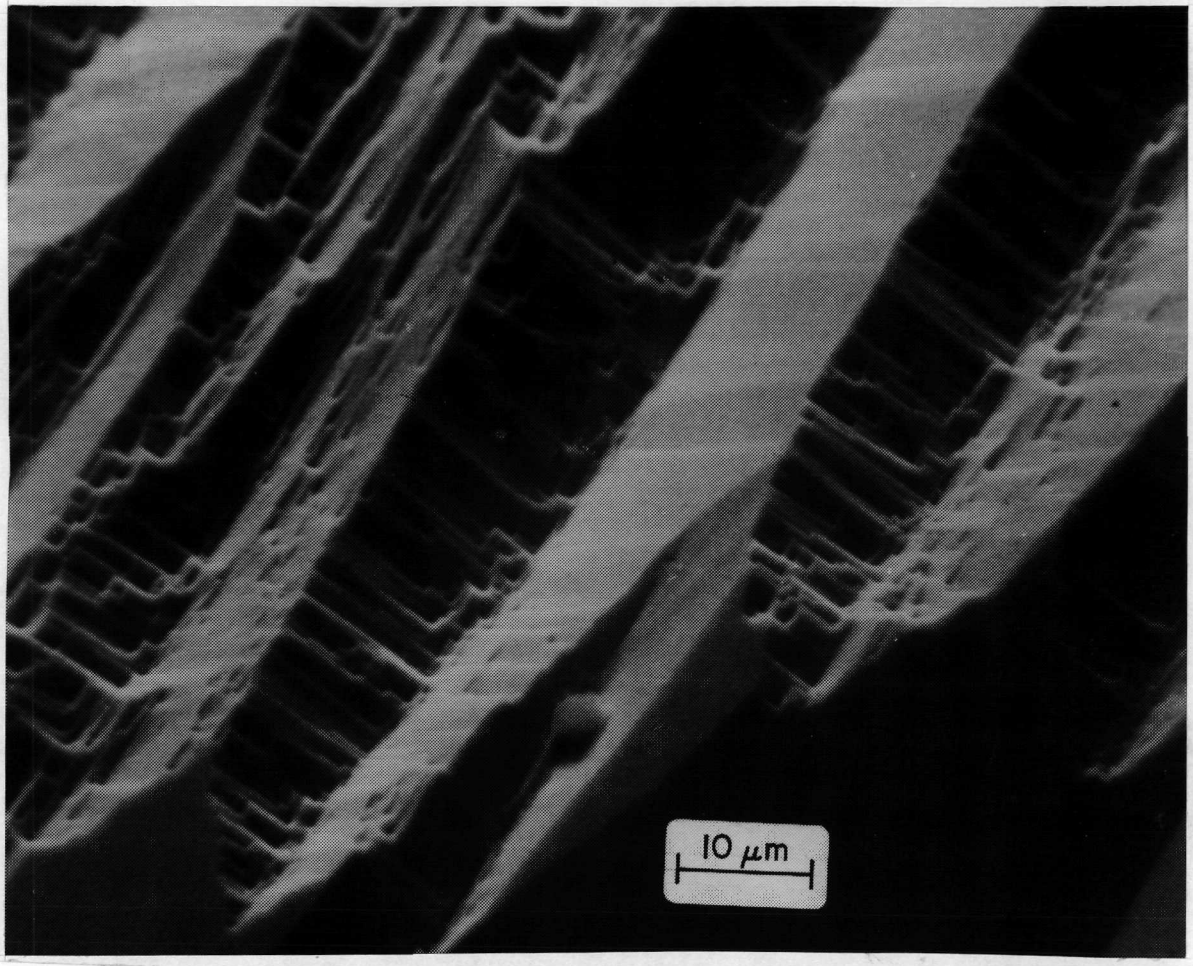

Figure 35. Scanning electron micrograph of GaN surface.

The following alternative models can be rejected for the reasons stated below:

1. Double injection: a) No near-gap emission is observed in Zn-doped GaN, indicating the absence of free holes. b) No emission is observed at the anode where holes would be injected.
2. Impact ionization: a) The emission spectrum, not limited by self-absorption, does not shift to higher energies with increasing excitation. b) There is no threshold breakdown voltage. c) The expected power dependence of the I-V characteristic is not obtained.

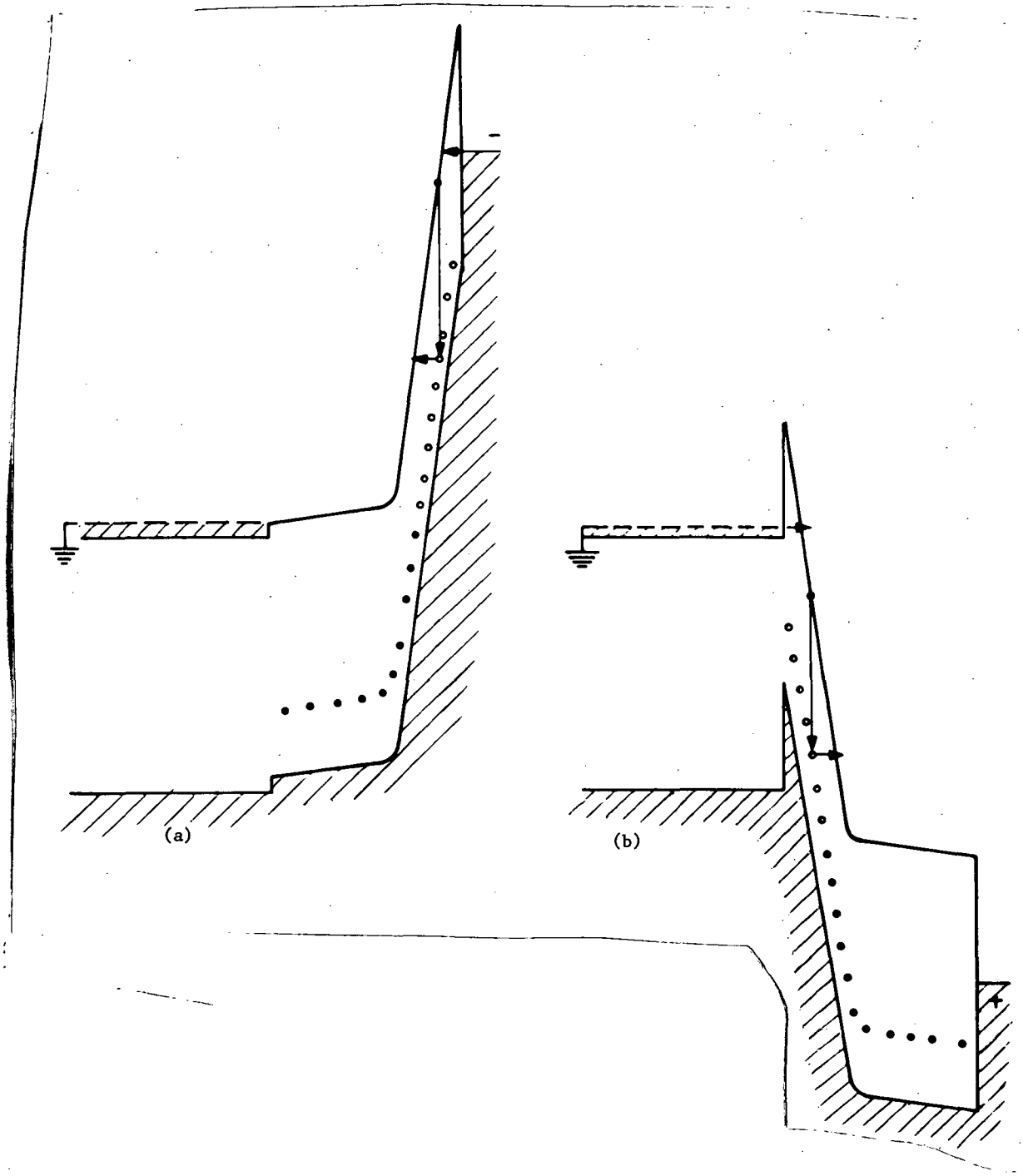

Figure 36. Model of the band structure for the M-i-n diode with (a) negative bias on M, (b) positive bias on M. Solid dots and circles are, respectively, ionized (filled) and neutral (empty) deep acceptors.

The model of localized field emission suggests that one should probe the potential distribution along the direction of the current flow. Such a measurement was done with a fine tungsten probe moved by a differential micrometer and connected to an electrometer. A position resolution of the order of 0.5 μm could be obtained. The potential profile across an M-i-n diode is shown in Fig. 37. With a positive bias on the In electrode, a rise in potential is obtained at the i-n transition where a sheet of light is observed. The thickness of the luminous sheet is difficult to determine because of the transparency of the crystal. When the polarity of the bias is reversed, a large potential drop appears at the M-i interface and light is emitted at this new position. The observed potential distribution is a necessary consequence of the proposed model of field concentration at the cathode.

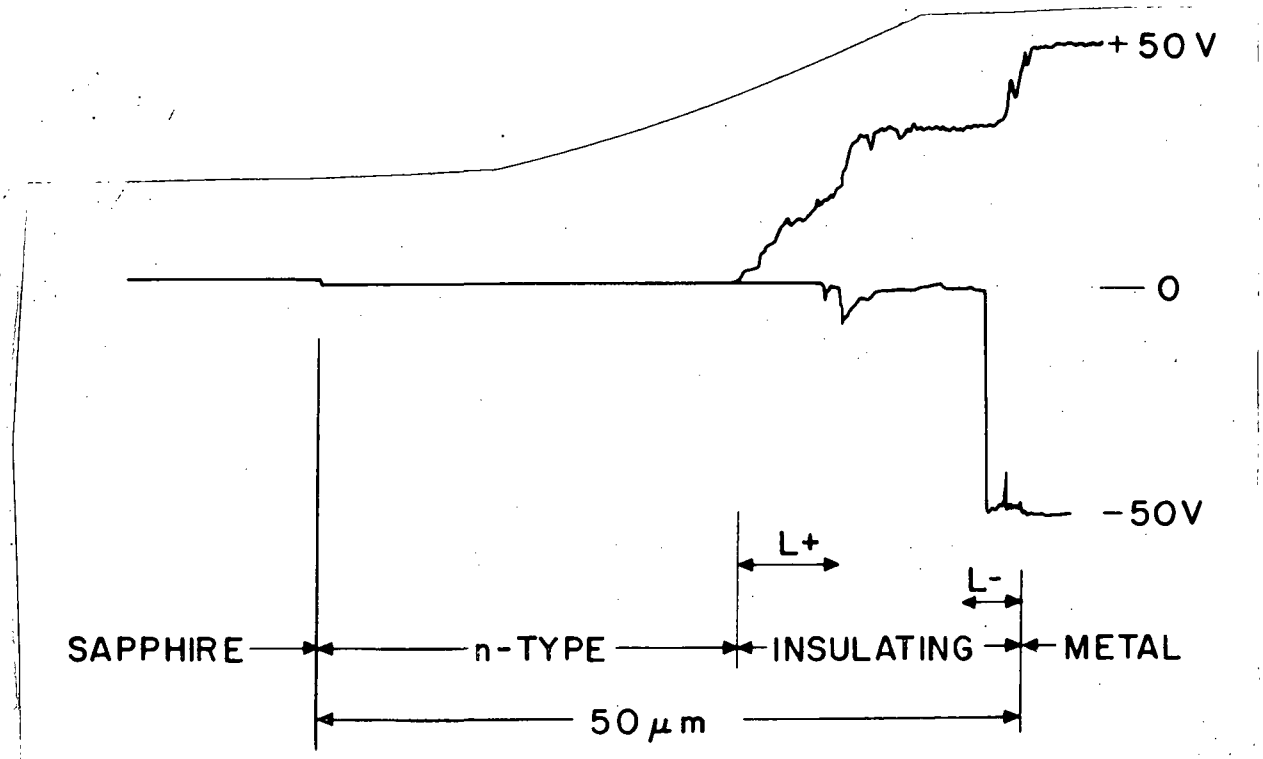

Figure 37. Potential profile probed along the M-i-n diode with both polarities of bias. The arrows show the position of the luminescent region during the indicated polarity.

Another consequence of the localization of the high field region is the relatively low quantum efficiency of the radiative process (low in contrast to the values obtainable with p-n junctions in other direct-gap compounds): the dwell time of the electron in the vicinity of the empty radiative center is short compared with the recombination time.

The thickness of the depletion region can be estimated by solving Poisson's equation for a 10-V drop in a region presumed to contain 10^{18} donor-acceptor pairs per cm^3. The result, 10^{-5} cm, would be in error only by a factor of about 3 if the pair concentration differed from 10^{18} by one order of magnitude. Assuming an electron velocity of 10^7 cm/sec*, the electron spends only about 10^{-12} sec in a region 10^{-5} cm thick. If the recombination time were of the order of 10^{-9} sec (as for the fundamental transition in GaAs), an emission efficiency of 10^{-3} would be expected. Admittedly, this is a rough order of magnitude estimate; but it is consistent with actual efficiency results. Actually, deep traps such as those responsible for luminescence in GaN should have very large capture cross sections, of the order of 10^{-14} cm^2, corresponding to a recombination time of 10^{-11} sec.

Further insight into the details of this model will depend on the proper interpretation of the luminescence delay mechanism and the I-V characteristics. The quadratic dependence of the I-V characteristic suggests a space-charge-limited current (SCLC) in the presence of traps (33). However, the SCLC mechanism could occur only near the anode since electrons are the majority carriers. We do observe a rise in potential at the anode when the metal is positive (Fig. 37) but not with the opposite polarization. Hence, it is difficult to conclude that we have two mechanisms operating simultaneously: 1) field emission and luminescence at the cathode, 2) SCLC at the anode controlling the I-V characteristic.

The luminescence delay could be due to thermal emptying of traps in the presence of a high electric field. When M is negative the high field would stabilize instantly at the cathode. When M is positive, electron extraction from the deep centers to M would induce a positive space charge at the M-i interface. This space charge would propagate in a few microseconds to the i-n interface, where it would stabilize.

Further thought and possibly further tests are needed before a definitive model will emerge. The final model may provide the long-sought explanation of electroluminescence in other materials, such as ZnS and ZnSe.

---

*P. D. Southgate of our Laboratories attempted a determination of the saturation velocity of electrons in undoped GaN from I-V characteristics using very short pulses. The material was ohmic up to 10^4 V/cm where the electron velocity was 7×10^6 cm/sec, setting this value as a lower limit for the saturation velocity. It is conceivable, however, that in Zn-doped GaN this limit could be lower.

VIII. NEW INSTRUMENTATION FOR TESTING LEDS

A test station was designed and built to record simultaneously the I-V characteristic and the dependence of the radiated power output on the electrical power input. Both of these curves were recorded as a log-log display. The circuit diagram for this test equipment is shown in Fig. 38.

As the dc bias across the diode was slowly increased, the voltage across the diode and the current through the i-n transition were sensed by logarithmic converters which fed their output ot an x-y plotter, thus generating a log I vs. log V display.

Simultaneously with the I-V measurement, the dependence of the electroluminescent output L_{out} on the input power P_{in} was recorded, also as a log-log plot. To obtain the L_{out} vs. P_{in} characteristic, the light emission of the diode was chopped and detected by a calibrated detector, the output of which was synchronously simplified and converted into its logarithmic value. The logarithm of the input power, P_{in}, was obtained by adding the output of the two logarithmic converters which are used to generate the I-V characteristics.

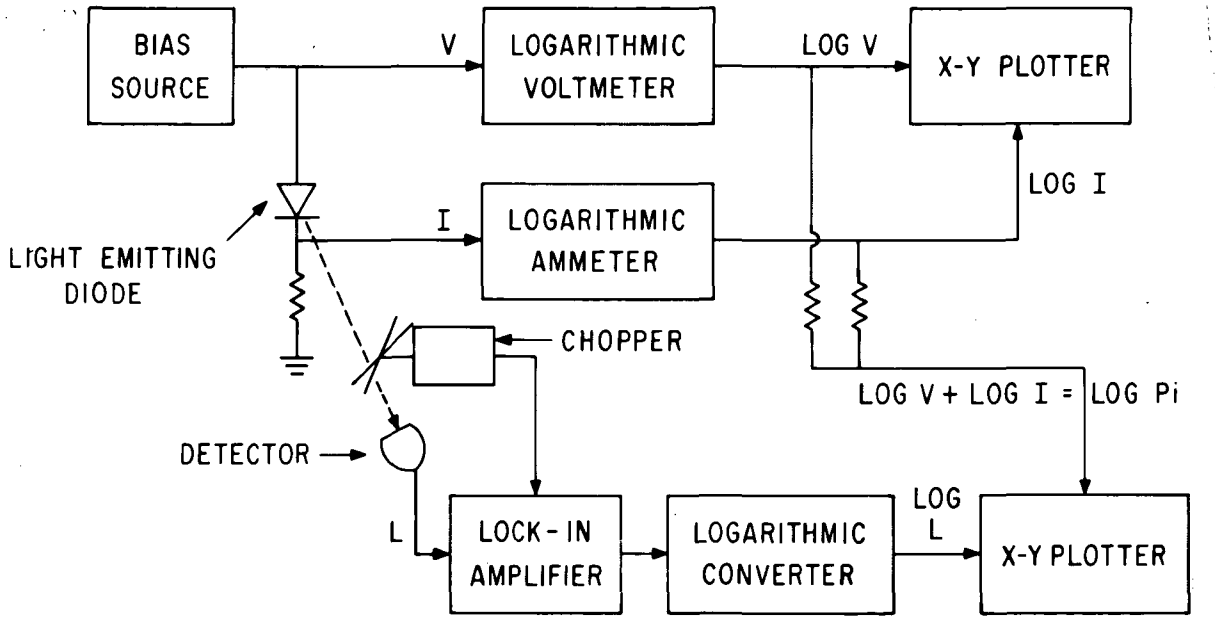

Figure 38. Schematic diagram of the setup for the measurement of GaN LED.

IX. CONCLUSIONS

GaN, which in the undoped condition is highly conducting and n-type, can be compensated by deep acceptors. These impurities can act as efficient radiative recombination centers emitting visible light. Be, Li, Mg, Dy, and Zn were found most effective in rendering GaN insulating.

By growing an insulating layer epitaxially on an undoped conducting layer, it was possible to make electroluminescent diodes emitting visible light continuously at room temperature. Zn-doping of the insulating layer was the object of our most intensive study. The partial pressure of the Zn vapor was varied during growth, the growth temperature was changed at constant Zn pressure, and the duration of growth was varied. From the accumulated data it appears that the best results are obtained when the crystal is grown in the 850° to 960° range with the Zn vapor pressure adjusted to barely overcompensate the native donors.

Electroluminescence was obtained over the blue to red range with Zn as the compensating impurity. The best results were obtained with emission in the blue-green at a 0.1% power efficiency. A brightness of 850 fL was achieved. A modulation at 70 MHz was possible by adding the modulation to a dc bias. In some diodes the color of the emitted light could be switched from red to green or red to yellow by reversing the polarity.

Valuable results were obtained by studying the luminescence properties of ion-implanted GaN.

A model was developed to account for some of the properties of electroluminescent diodes: field emission of electrons from deep centers as the cathode leaves empty (neutral) deep acceptors which have a large capture cross section for radiative transition. The field is localized at the cathode by sharp points resulting from the texture of microfacets.

Much work still remains to be done before GaN reaches its ultimate potential as a practical source of electroluminescence. The growth parameters need further optimization, especially concerning the choice of substrate to minimize lattice mismatch and interfacial strain. The properties of other impurities must be explored in our search for p-type GaN. Further insight must be gained in the operation of the GaN LED through a study of the kinetics of radiative recombination (delay effects and recombination time) and a study of the temperature dependence of electrical and optical properties. Eventually the properties of related compounds should be explored: $In_{1-x}Ga_xN$, $Al_{1-x}Ga_xN$, and $In_{1-x}Al_xN$.

REFERENCES

1. H. P. Maruska and J. J. Tietjen, Appl. Phys. Letters 15, p. 327 (1969).
2. J. I. Pankove, J. E. Berkeyheiser, H. P. Maruska, and J. P. Wittke, Solid State Commun. 8, 1051 (1970).
3. J. I. Pankove, H. P. Maruska, and J. E. Berkeyheiser, Appl. Phys. Letters 17, 197 (1970).
4. D. Camphausen and G. A. N. Connell, J. Appl. Phys. 42, 4438 (1971).
5. S. Bloom, J. Phys. Chem. Solids 32, 2027 (1971).
6. R. Dingle and M. Ilegems, Solid State Commun. 9, 175 (1971).
7. R. D. Cunningham, R. V. Brander, N. D. Knee, and D. K. Wickenden, J. Luminescence 5, 21 (1972).
8. G. Harbecke (unpublished).
9. J. I. Pankove, E. A. Miller, and J. E. Berkeyheiser, Proc. 10th Int. Conf. Phys. Semiconductors, 1970, USAEC, p. 593.
10. J. I. Pankove, D. Richman, E. A. Miller, and J. E. Berkeyheiser, J. Luminescence 4, 63 (1971).
11. J. I. Pankove, E. A. Miller, and J. E. Berkeyheiser, J. Luminescence 5, 84 (1972).
12. J. I. Pankove, E. A. Miller, and J. E. Berkeyheiser, RCA Review 32, 383 (1971).
13. J. I. Pankove, E. A. Miller, and J. E. Berkeyheiser, J. Luminescence 6, 54 (1973).
14. J. I. Pankove, J. Luminescence 5, 482 (1972).
15. J. I. Pankove and P. S. Norris, RCA Review 33, 377 (1972).
16. J. I. Pankove, J. Electrochem. Soc. 119, 1118 (1972).
17. V. S. Ban, J. Electrochem. Soc. 119, 761 (1972).
18. R. Juza and H. Hahn, Z. Anorg. Allgem. Chem. 239, 282 (1938).
19. R. Paff, private communication.
20. M. Ilegems and R. Dingle, J. Appl. Phys. (to be published).
21. M. Ilegems, R. Dingle, and R. A. Logan, J. Appl. Phys. 43, 3797 (1972).
22. R. E. Honig and D. A. Kramer, RCA Review 30, 285 (1969).
23. H. P. Maruska, W. C. Rhines, and D. A. Stevenson, Materials Res. Bull. 7, 777 (1972).
24. J. P. Maruska, D. A. Stevenson, and J. I. Pankove, Appl. Phys. Letters 22, 303 (1973).

25. H. M. Manasevit, F. M. Erdman, and W. I. Simpson, J. Electrochem. Soc. 118, 1864 (1971).

26. M. T. Duffy, C. C. Wang, G. D. O'Clock, Jr., S. H. McFarlane III, and P. J. Zanzucchi, J. Electronic Materials 2, 359 (1973).

27. H. G. Grimmeiss and H. Koelmans, Z. Naturforsch. 14a, 264 (1959).

28. H. G. Grimmeiss, R. Groth, and J. Maak, Z. Naturforsch. 15a, 799 (1960).

29. H. F. Gossenberger, private communication.

30. E. W. Williams, private communication.

31. J. I. Pankove, Phys. Rev. 140, A2059 (1965).

32. R. D. Cunningham, R. W. Brander, N. D. Knee, and D. K. Wickenden, J. Luminescence 5, 21 (1972).

33. M. Lampert and P. Mark, Current Injection In Solids, (Academic Press, New York, 1970).